Trust Failures and Decarbonization *

Varun Kapoor †

October 14, 2026

Abstract

Electric two-wheelers offer a promising path to decarbonizing transport in lower- and middle-income countries, but uncertainty about product reliability and after-sales service may slow their adoption. We examine whether the 2024 service-quality crisis at Ola Electric, then India's largest electric two-wheeler manufacturer, affected demand for non-Ola electric vehicles. To determine whether the crisis affected adoption beyond Ola, we exploit geographic variation in the firm's pre-crisis installed base using administrative registration data from 886 Regional Transport Offices. A triple-difference design compares non-Ola electric two-wheelers with internal-combustion two-wheelers within the same local market, while synthetic difference-in-differences compares highly exposed markets with weighted lower-exposure markets that followed similar pre-crisis trajectories. After the crisis, non-Ola electric registrations grew more slowly relative to internal-combustion registrations in places with higher pre-study window exposure to Ola sales. In the most exposed markets, non-Ola registrations were 17 percent below their synthetic counterfactual during the following year, and total electric registrations were 12 percent lower. Rather than shifting demand toward competitor brands, the market leader's service failures degraded consumer confidence in the technology category as a whole. These findings demonstrate that firm-level service reliability and brand reputation directly constrain clean-technology diffusion, exposing structural vulnerabilities in transition policies that concentrate rapid expansion among a small cohort of early movers.

Keywords: electric vehicles; technology adoption; collective reputation; consumer trust.

JEL codes: L14, L15, L62, O33, Q48, Q55.

*The IRB approval for this project was provided by Harvard University.

†Harvard University: varun_kapoor@fas.harvard.edu

1 Introduction

In many lower- and middle-income countries scooters and motorcycles account for a large share of personal mobility vehicles, making two-wheelers a central segment of the transition to electric transport. Two-wheelers may also be relatively well suited to electrification as the absolute upfront premium for electric models is typically smaller than for four-wheelers, and lower operating costs can recover that premium more quickly (Briceno-Garmendia et al., 2022). Realizing this potential requires understanding what prevents households from choosing electric vehicles. India has set a target for electric vehicles to reach 80% of new two- and three-wheeler sales by 2030 (NITI Aayog and Rocky Mountain Institute, 2019). Whether such ambitions can be realized depends on addressing the barriers to adoption.

Much of the quantitative literature on EV adoption emphasizes high upfront prices and limited charging infrastructure. Li et al. (2021) attribute about 17% of the cross-country adoption gap to purchase subsidies and 69% to charging networks, and related work documents the importance of policy incentives and charging externalities (Li et al., 2017; Springel, 2021; Rapson and Muehlegger, 2023). Another important margin is whether buyers trust the new technology and the firms that sell and service it. Vehicle purchases represent a major investment for many households in these countries, so concerns about reliability, service quality, or the durability of a new technology may discourage adoption even when its financial costs are otherwise attractive. However, it is difficult to empirically assess how trust in technology shapes electric-vehicle adoption, and direct evidence on this channel remains limited.

We try to answer this question by studying whether a loss of trust in a market leader, triggered by visible service failures, can slow the adoption of an emerging clean technology by reducing demand for competing producers in the same category. In nascent EV markets, consumers have limited experience with the technology, and their confidence may depend partly on the reputations of the firms that produce and service it. Failures at a prominent producer may therefore shape beliefs about the broader technology and the service ecosystem that supports it. We investigate these potential spillovers using the 2024 service-quality crisis at Ola Electric, then India's largest electric two-wheeler manufacturer.

Ola accounted for a reported 52% of India's electric two-wheeler market in April 2024. Between mid-September and early October, a sequence of public reports brought concerns about its product reliability and after-sales service capacity to national attention. On 18 September, a national newspaper reported an estimated $80{,}000$ service complaints per month (Mint, 2024). In a September client note, HSBC analysts reported that most Ola service centres they visited were overwhelmed by service requests (Reuters, 2024). On 7 October, the national consumer regulator issued a formal notice citing $10{,}644$ verified complaints (Business Standard, 2024). By February 2025, Ola's reported market share stood at approximately 19%. We use September 2024 to date the public emergence of the service crisis and examine whether the ensuing weakness extended to competing electric two-wheeler producers.

The demand response for competing electric brands distinguishes two possible consequences

of the crisis. If consumers viewed the service failures as specific to Ola, other electric manufacturers could have gained customers switching away from the firm. If consumers instead treated Ola's problems as informative about electric two-wheelers or their supporting service ecosystem, demand for competing electric brands could also have weakened. Evidence from product-recall and product-harm studies shows that firm-specific failures can affect competitors (Jarrell and Peltzman, 1985; Freedman et al., 2012; Borah and Tellis, 2016; Van Heerde et al., 2007), but much of this evidence concerns mature product markets. Our question is whether such spillovers can impede the adoption of an emerging clean technology.

We exploit geographic variation in Ola's presence before the crisis to study differences in its local effects. Although the public revelations were national, their local relevance may have varied with the number of Ola vehicles already in use. A larger installed base could give prospective buyers more opportunities to encounter owners' service experiences and observe failures in the local service network. This motivates using Ola's pre-crisis installed base to measure local exposure to the shock. We ask whether non-Ola electric registrations subsequently weakened more in markets where Ola had been more established.

We use administrative data from VAHAN, India's national vehicle-registration platform, which reports new registrations by Regional Transport Office (RTO), manufacturer, vehicle type, and month (Ministry of Road Transport and Highways, 2026). RTOs administer vehicle registration within defined geographic jurisdictions and serve as our local market units. Our sample contains 886 RTOs observed from December 2023 through August 2025, with September 2024 as the first treatment month. We measure exposure as the logarithm of one plus cumulative Ola two-wheeler registrations from April 2022 through November 2023. This window ends before the outcome panel begins and nine full months before the treatment month. This construction follows the logic of exposure designs that use pre-period characteristics to capture local treatment intensity (Autor et al., 2013; Acemoglu et al., 2016).

A national before-and-after comparison is difficult to interpret because the crisis coincided with changes in India's EV subsidy regime. We therefore implement a triple-difference design comparing before versus after the crisis, non-Ola electric versus internal combustion engine (ICE) two-wheelers, and RTOs with greater versus smaller pre-crisis Ola exposure. It asks whether non-Ola electric registrations weakened relative to ICE registrations more in markets with a larger Ola installed base. The specification accounts for persistent local differences between the segments, monthly local shocks common to both segments, and national monthly changes specific to each segment, including EV subsidy changes. Our preferred specification also allows pre-crisis total two-wheeler market size and growth to predict different post-crisis changes across segments. Identification requires that, absent the crisis and conditional on these adjustments, the non-Ola-electric-versus-ICE registration gap would have evolved similarly across markets with different Ola exposure.

Our second approach, synthetic difference-in-differences, compares electric registrations across markets without using ICE registrations as a benchmark. We classify the 221 RTOs in the top

quartile of Ola exposure as high-exposure markets and construct a weighted comparison from the remaining 665 RTOs using their pre-crisis registration paths (Arkhangelsky et al., 2021). The identifying assumption is that, absent the crisis, the high-exposure group and its weighted comparison would have maintained their pre-crisis relationship. Both designs estimate differences in the response across more- and less-exposed markets; any effect common to all markets is absorbed by their time comparisons.

The triple-difference estimates show that non-Ola electric registrations weakened relative to ICE registrations after the crisis as pre-crisis Ola exposure increased. In the preferred specification, the difference between mean exposure in the bottom and top quartiles implies an approximately 34% relative shortfall in non-Ola electric registrations over the first post-crisis year. This magnitude describes the change in non-Ola registrations relative to ICE registrations across that exposure contrast.

The synthetic difference-in-differences estimates show that non-Ola electric registrations in the top-quartile exposure group were approximately 17% below their synthetic counterfactual from September 2024 through August 2025. This compares the top quartile with a weighted combination of the lower three quartiles using electric registrations alone, so it measures a different contrast from the triple-difference estimate. Total electric registrations, including Ola, were approximately 12% below their separately estimated synthetic counterfactual. Each outcome receives its own comparison weights, so the total-electric estimate is not a mechanical combination of the non-Ola estimate and Ola's own decline.

The timing evidence helps distinguish the crisis response from earlier changes in EV demand. In the baseline event study, exposure-related differences are visible around the early-2024 subsidy transition, followed by a relatively stable period immediately before the crisis. The coefficients become negative in September 2024 and remain negative through August 2025. To assess whether this pattern reflects broader local EV-market movements, we also compare non-Ola electric two-wheelers with four-wheeler EVs, a segment in which Ola did not operate. In that comparison, the pre-crisis coefficients are close to zero and the negative differential emerges in September. The main result also survives allowing segment-specific monthly paths across regions and excluding July and August 2024, when Ola's own registrations had already begun to decline.

The estimates describe a slowdown relative to the counterfactual rather than an absolute contraction of the electric market. Non-Ola electric registrations continued to grow in high-exposure RTOs, but they grew more slowly than in comparable lower-exposure markets. Ola's own registrations fell sharply, while total electric registrations and the electric-to-ICE registration ratio also weakened with pre-crisis Ola exposure. Consequently, the electric share of two-wheeler registrations remained approximately constant at 11% in the most exposed RTOs, while rising from 4.8% to 5.9% elsewhere. We find no statistically detectable differential increase in ICE registrations, although the estimates are not precise enough to determine whether the missing electric purchases shifted to ICE vehicles or were postponed altogether.

We then examine whether the rival-registration shortfall is related to pressure on Ola's local

service network. Using archived January 2024 service-centre locations and the pre-crisis Ola fleet, we construct an estimated service load: the average number of installed Ola vehicles assigned per workshop across the workshops serving each district. This measures potential pressure on service capacity rather than observed waiting times. Conditional on baseline Ola exposure, non-Ola electric registrations weaken more relative to ICE registrations in markets with higher estimated service load. There is no detectable differential before the crisis. This pattern links the weakness among competing brands to local service-network strain beyond the size of Ola's installed base.

Taken together, the findings are consistent with a category-level reputational spillover. Non-Ola electric registrations grew more slowly after the crisis in markets where Ola had been more established, and the shortfall was subsequently larger where its service network faced greater estimated pressure. These patterns accord with consumers treating a prominent producer's service failures as informative about electric two-wheelers and their supporting service ecosystem. The resulting slowdown in electric adoption makes service reliability relevant to decarbonization policy: purchase subsidies and charging infrastructure may be less effective when rapid adoption is not accompanied by reliable products, adequate repair capacity, and credible consumer protection.

Related literature. The paper draws on two lines of work. The first studies how reputation and information shape demand when buyers cannot directly observe quality. Tirole (1996) provides a theory of collective reputation, while Shapiro (1983) shows how reputation can support high-quality provision when quality is not immediately observed. Cabral and Hortaçsu (2010) document reputation dynamics in eBay data, and Jin and Leslie (2003) show that public quality disclosure shifts demand toward higher-quality sellers. The same logic appears in durable-goods markets, where uncertainty about quality can depress demand or change resale patterns (Akerlof, 1970; Bond, 1982; Genesove, 1993; Hendel and Lizzeri, 1999; Lewis, 2011). Closest to our result is the product-recall and product-harm literature: one firm's failure can lower its own value, affect rivals, and alter consumers' responses to brands (Jarrell and Peltzman, 1985; Rhee and Haunschild, 2006; Freedman et al., 2012; Dawar and Pillutla, 2000; Van Heerde et al., 2007; Cleeren et al., 2008; Borah and Tellis, 2016). Bachmann et al. (2023) use the 2015 Volkswagen emissions scandal to show that a shock to one firm spilled to other German diesel brands, reallocating demand across producers within a mature product category. Bai et al. (2022) document the same force in a developing-country export setting: after the 2008 melamine scandal, Chinese dairy exporters without contaminated products lost export revenue alongside the contaminated firms, as foreign buyers pooled producers under a shared origin label. We extend this literature to the adoption of an emerging clean technology. The relevant margin is whether a leading producer's failure slows the expansion of electric vehicles relative to incumbent combustion vehicles. By examining competing electric producers and the electric category as a whole, we connect firm-level reputational spillovers to the pace of the transport transition.

The second line studies demand for electric vehicles and clean vehicle technologies. Adoption responds to purchase incentives, fuel prices, and charging networks (Gallagher and Muehlegger,

2011; Li et al., 2017, 2021; Springel, 2021; Rapson and Muehlegger, 2023), while the environmental gains depend on which ICE vehicles EVs replace and on the local emissions intensity of electricity generation (Xing et al., 2021; Holland et al., 2016). In lower-income countries, two- and three-wheelers often have the clearest economic case for electrification (Briceno-Garmendia et al., 2022). Less wealthy buyers can be highly price-responsive (Muehlegger and Rapson, 2022), and survey evidence from India points to price, charging access, market visibility, and social influence as important determinants of electric two-wheeler adoption (Chakraborty and Chakravarty, 2023; Bhat and Verma, 2024). Consumer-perception studies also highlight perceived risk, performance, and technology familiarity as barriers to EV adoption (Egbue and Long, 2012; Rezvani et al., 2015). This literature usually treats firm reputation and service quality as fixed or unobserved. We provide causal evidence from a reputational shock to a leading producer.

The paper proceeds as follows. Section 2 describes the market and the service crisis. Section 3 presents the data, identification strategies, and adoption results. Section 4 examines the evidence linking these results to service-network congestion. Section 5 concludes.

2 Setting

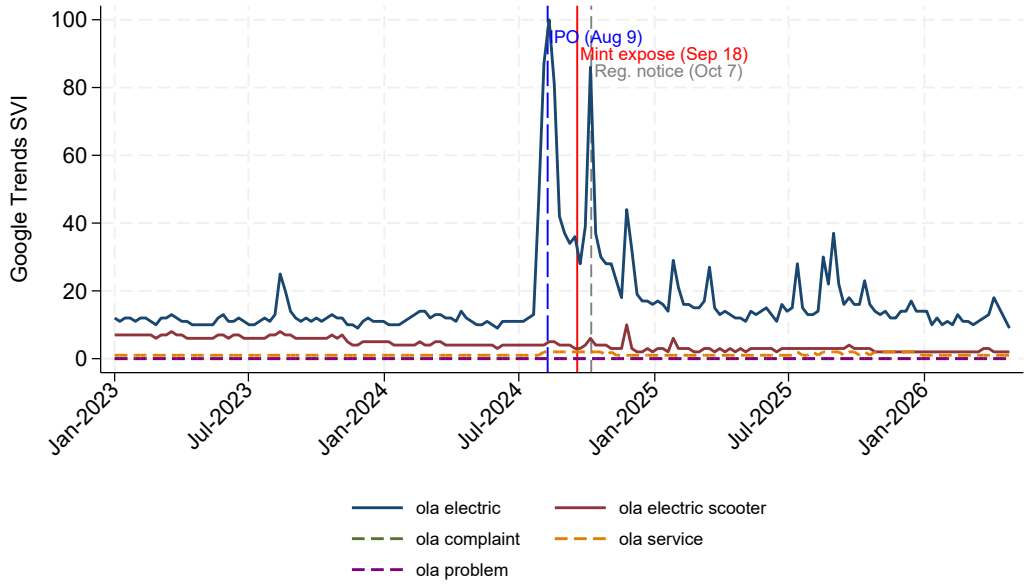
India's high-speed electric two-wheeler segment expanded rapidly after 2020, supported in part by central-government purchase incentives. Ola Electric emerged as the dominant producer. By April 2024, Ola reportedly accounted for 52% of new high-speed electric two-wheeler registrations, while the next-largest competitors—TVS Motor, Bajaj Auto, Ather Energy, and Hero MotoCorp's Vida brand—held single-digit or low double-digit shares.

Three events between mid-September and early October 2024 brought service-quality concerns to public attention. On 18 September 2024, the Indian business newspaper *Mint* published an exposé citing internal documents to estimate $\sim 80{,}000$ monthly service complaints across Ola's installed base (Mint, 2024). In a September client note, HSBC analysts who visited Ola service hubs reported that most "appeared overwhelmed by the service requests", attributing the strain to under-investment in service capacity relative to the volumes the firm had sold (Reuters, 2024). On 7 October 2024, the Central Consumer Protection Authority of India issued a formal show-cause notice based on $10{,}644$ verified consumer complaints (Business Standard, 2024). We treat September 2024 as the first month in which the crisis became publicly salient. Because private information about service failures may have diffused before the national reports, we also report a donut robustness check that drops July and August 2024 from the estimation window.

Evidence on public salience. Figure 1 plots weekly Google search volume in India for "ola electric" and several complaint-related terms. Searches for the brand rose sharply around the firm's August 2024 stock-market listing and again during the September–October service-crisis period. The complaint-specific terms remained at or near Google's reporting threshold. Accordingly, the figure provides evidence that the Ola brand became more salient during the crisis, but it does not

establish that consumers searched specifically for complaint-related information. The timing is nevertheless consistent with the adverse public information reaching an audience beyond existing Ola owners.

Figure 1: Weekly Google search salience of Ola Electric in India

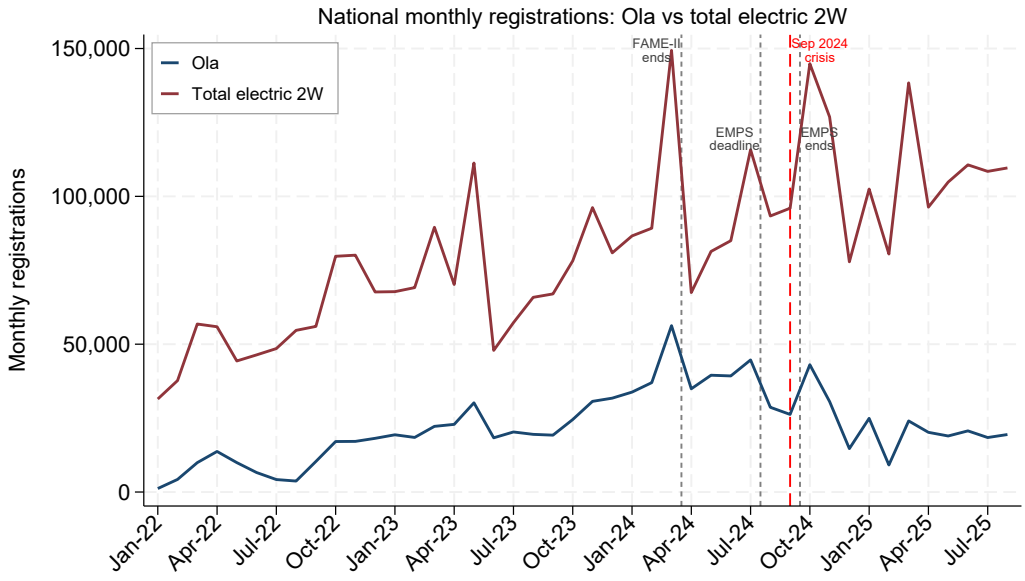


Notes: Weekly Google Trends search-volume index for India, normalised so that 100 is the maximum value across the displayed series within the sample window. The solid line marks the *Mint* exposé on 18 September 2024, and the dashed line marks the regulator's show-cause notice on 7 October 2024. The three complaint-related terms ("ola complaint", "ola service", and "ola problem") remain at or near zero because their absolute search volume is below Google's reporting threshold.

The decline of Ola Electric. Figure 2 documents the firm's national registration trajectory. It plots monthly Ola electric two-wheeler registrations alongside total high-speed electric two-wheeler registrations, aggregated across all RTOs. Ola registrations peaked in early 2024 and declined during the remainder of the year, while the total electric two-wheeler market continued to expand; consequently, Ola's category share fell as non-Ola brands grew. The red dashed line identifies September 2024, the month used to date the reputational shock. The pre-shock geographic distribution of Ola's installed base provides the cross-sectional variation used in Section 3.

An aggregate event study to identify the spillover? An aggregate before-and-after comparison cannot isolate the effect of Ola's crisis because the crisis coincided with major changes in India's national EV subsidy regime. One could, in principle, compare national registrations of non-Ola electric two-wheelers with those of ICE two-wheelers before and after September 2024. For this comparison to identify the spillover from Ola, however, no other contemporaneous event could differentially affect demand for electric two-wheelers. This condition is not satisfied: the months

Figure 2: National Ola registrations and the total electric two-wheeler market



Notes: National monthly registrations of Ola electric two-wheelers (navy) and all high-speed electric two-wheelers (maroon, $=$ *Ola* $+$ *non-Ola E2W*), aggregated across all RTOs rather than restricted to the size-filtered estimation sample. Grey dashed lines mark the end of FAME-II (31 March 2024), the original EMPS deadline (31 July 2024), and the extended end of EMPS (30 September 2024). The red dashed line marks September 2024, the treatment month. Ola's share of high-speed electric two-wheelers declined from approximately 52% in April 2024 to about 18% by the end of the displayed period, while total market registrations continued to increase.

surrounding the crisis saw several changes in the central government's purchase incentives for electric vehicles, and electric two-wheeler registrations closely track the timing of these incentives (Mobility Outlook, 2024).

The first major change occurred several months before the crisis. Phase II of the Faster Adoption and Manufacturing of (Hybrid &) Electric Vehicles in India scheme (FAME-II), the central government's principal EV purchase-subsidy programme, expired on 31 March 2024. It was replaced on 1 April by the Electric Mobility Promotion Scheme (EMPS), under which the per-vehicle incentive for electric two-wheelers was approximately halved (Ministry of Heavy Industries, 2019, 2024a). The expiration of FAME-II generated a pull-forward of purchases into March, followed by a trough in April. EMPS was initially scheduled to expire on 31 July, creating another incentive to purchase before the deadline, but the government extended the scheme on 26 July through 30 September (Ministry of Heavy Industries, 2024a). These changes in anticipated subsidy deadlines contributed to the summer peak in electric two-wheeler registrations shown in Figure 2.

A second policy transition occurred almost exactly when Ola's service crisis became publicly salient. The PM Electric Drive Revolution in Innovative Vehicle Enhancement scheme (PM E-DRIVE), which succeeded EMPS, was approved on 11 September, notified on 29 September, and implemented on 1 October (Ministry of Heavy Industries, 2024c). This transition did not reduce

the headline subsidy available to electric two-wheeler buyers: both EMPS and PM E-DRIVE offered Rs. 5,000 per kWh, capped at Rs. 10,000 per vehicle during PM E-DRIVE's first year, with the scheduled reduction beginning only in April 2025 (Ministry of Heavy Industries, 2024a,c; Autocar Professional, 2024c). Nevertheless, the transition changed the timing and expected duration of government support. PM E-DRIVE replaced a programme approaching its 30 September expiry with a larger two-year scheme covering electric vehicles and charging infrastructure (Ministry of Heavy Industries, 2024c; Autocar Professional, 2024b). By removing the immediate expiry deadline, the new programme may have reduced the incentive to bring purchases forward to the end of September. Trade reporting attributed weak September sales partly to this reduced urgency and partly to a religiously inauspicious period (Autocar Professional, 2024a).

The national electric-versus-ICE time series therefore reflects both the potential effect of Ola's reputational crisis and contemporaneous policy-induced changes in electric two-wheeler demand. Because the Ola crisis and the transition to PM E-DRIVE occurred at essentially the same time, a national event study cannot distinguish between them.

We therefore exploit cross-sectional variation in predetermined local exposure to Ola. Rather than attributing the national change in electric registrations after September 2024 to the crisis, we ask whether electric outcomes changed more in RTOs where Ola had a larger installed base before the shock. National policy changes cannot by themselves generate such an exposure gradient. They remain a threat to identification only if their effects differ systematically across RTOs in ways that are correlated with pre-crisis Ola exposure. Section 3 formalizes this identifying assumption and examines it empirically.

3 Empirical analysis

3.1 Data, sample construction, and timing

We use administrative data from VAHAN, India's national vehicle-registration platform (Ministry of Road Transport and Highways, 2026). The data report monthly counts of new registrations by Regional Transport Office (RTO), manufacturer, and vehicle type. We restrict attention to scooters and motorcycles, the vehicle classes that contain high-speed electric two-wheelers and their internal-combustion-engine (ICE) alternatives. From these records, we construct four mutually consistent series for each RTO-month: Ola electric two-wheelers, non-Ola electric two-wheelers, ICE two-wheelers, and total high-speed electric two-wheelers, where the last category is the sum of Ola and non-Ola registrations. Registrations, rather than vehicle purchases, are therefore the outcome throughout the analysis.

RTOs are government authorities that register vehicles within defined geographic jurisdictions. We use an RTO as a proxy for a local vehicle market because it is the finest geographic unit consistently available in the registration data. One limitation is that the data do not identify purchases made across RTO boundaries. To exclude very small and noisy markets, we retain RTOs with at least 100 cumulative high-speed electric two-wheeler registrations and at least $2{,}000$ cu-

mulative two-wheeler registrations, electric and ICE combined, between April 2022 and November 2023. The resulting sample contains 886 RTOs across 27 Indian states and union territories.

The timing separates sample construction and exposure measurement from the outcomes used to estimate the effects of the crisis. We use April 2022–November 2023 to select the RTO sample and to measure each market's predetermined Ola exposure. The regression panel begins only in December 2023, leaving nine full months between the end of the exposure window and the treatment month. Within that panel, December 2023–August 2024 forms the nine-month pre-crisis period. We date the shock to September 2024, when public reports of Ola's service problems first appeared; because those reports began in the middle of the month, September is a partially exposed first post-crisis month. The post-crisis period then runs from September 2024 through August 2025.

These data are organized differently for the two empirical designs. The triple-difference analysis stacks non-Ola electric and ICE registrations within each RTO-month and asks whether their relative post-crisis path varies with predetermined Ola exposure. The synthetic difference-in-differences analysis instead uses RTO-month outcomes and compares non-Ola or total electric registrations in high-exposure RTOs with weighted lower-exposure RTOs. The next subsection defines exposure and the identifying comparisons formally.

3.2 Identification strategy

Continuous exposure measure. For each RTO r, predetermined Ola exposure is defined as

$$\textit{Ola Exposure}_r = \log\left(1 + \sum_{t=\text{Apr 2022}}^{\text{Nov 2023}} \textit{Ola}_{rt}\right), \tag{3.1}$$

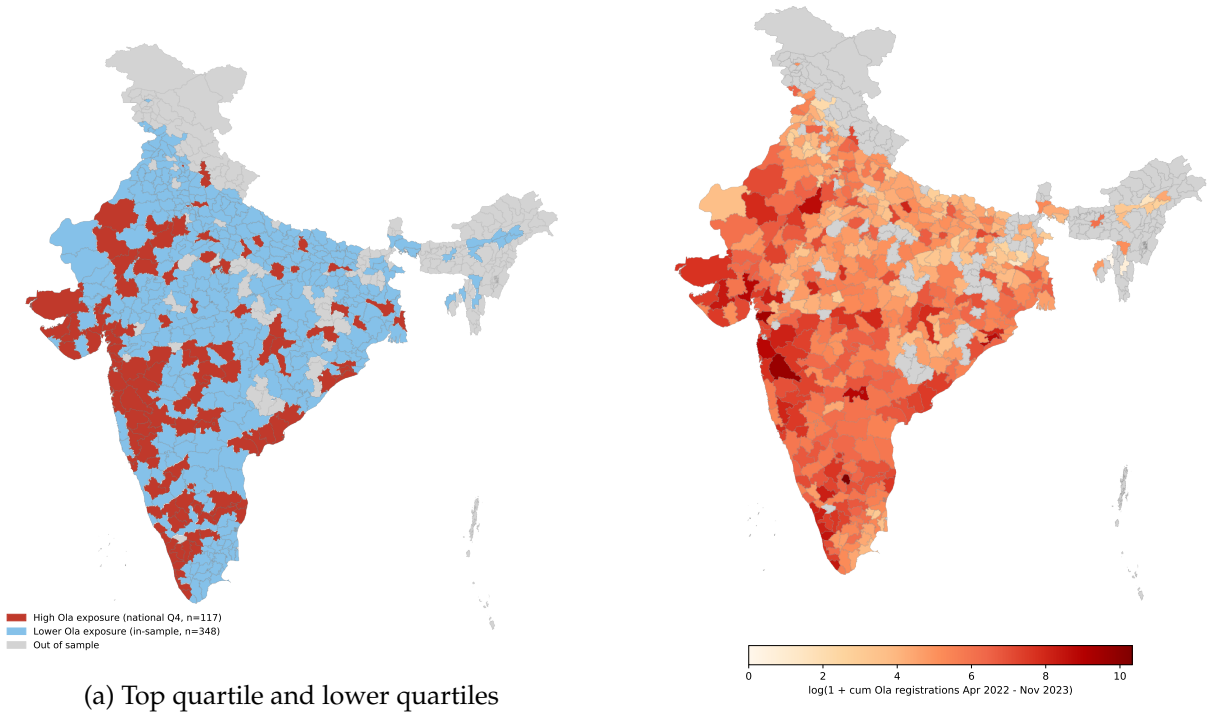
that is, the natural logarithm of one plus cumulative Ola two-wheeler registrations in the RTO from April 2022 through November 2023.

This measure has three advantages. First, the exposure window ends before the regression panel begins and nine full months before the treatment month, so it excludes observations used to estimate pre-trends or post-shock outcomes. Second, an absolute installed-base measure is more stable than a share with a changing denominator in a rapidly expanding two-wheeler market. Third, the logarithmic transformation reduces skewness and the influence of very high-exposure RTOs.

Geographic distribution of exposure. Figure 3 presents the pre-shock geographic distribution of Ola registrations, aggregating RTOs to Census 2011 districts. Panel (a) identifies in red the districts in the nationwide top quartile of $\log(1 + \textit{cum Ola})$, and Panel (b) displays the continuous measure. Exposure is concentrated in southern India (Karnataka, Tamil Nadu, Kerala, Telangana, and Andhra Pradesh), along the western coast (Maharashtra, Goa, and Gujarat), and around Delhi and Bangalore. It is lower in the eastern states (Bihar, Odisha, West Bengal, and the North East)

and in the Hindi heartland (Uttar Pradesh and Madhya Pradesh).

Figure 3: Pre-shock Ola exposure across Indian districts



(a) Top quartile and lower quartiles

(b) Continuous $\log(1 + \textit{cum Ola})$ measure

Notes: District-level aggregation of RTO-level *Ola Exposure*$_r$ from Equation (3.1), measured over April 2022–November 2023. Each in-sample RTO is mapped to its Census 2011 district; the match rate is 97.6% and covers 99.6% of cumulative Ola registrations. In Panel (a), red districts are in the nationwide top quartile of district-level $\log(1 + \textit{cum Ola})$, and blue districts are the remaining in-sample districts. Panel (b) displays the same measure continuously. Districts without a matched in-sample RTO are shown in grey.

Design 1: triple-difference. The first design stacks two segments within each RTO-month: *non-Ola electric two-wheelers*, defined as all electric two-wheeler registrations excluding Ola, and *ICE two-wheelers*. Let $f \in \{\text{Non-Ola electric, ICE}\}$ index the segment. We estimate

$$\begin{aligned}\log(\textit{Registrations}_{rft} + 1) = \alpha_{rf} + \mu_{rt} + \delta_{ft} \\ + \sum_{\tau \neq -1} \beta_\tau \cdot (\textit{Ola Exposure}_r \cdot \mathbf{1}[t - \text{Sep '24} = \tau] \\ \cdot \mathbf{1}[f = \text{Non-Ola electric}]) + \varepsilon_{rft}.\end{aligned} \tag{3.2}$$

The fixed effects α_{rf} (RTO $\times$ segment) absorb permanent differences in segment levels within each RTO. The fixed effects μ_{rt} (RTO $\times$ month) absorb all local time-varying factors that affect the two segments equally within an RTO-month, including common local demand, infrastructure, administrative, or competitive shocks. The fixed effects δ_{ft} (segment $\times$ month) absorb segment-

specific national time paths, including the differential evolution of electric and ICE two-wheelers and segment-specific seasonality. The coefficients β_τ are therefore identified by the remaining within-RTO-month variation: the change in non-Ola electric registrations relative to ICE registrations along the predetermined Ola-exposure gradient.

The static specification replaces the event-time indicators with $Post_t = \mathbf{1}[t \geq \text{Sep 2024}]$. We also estimate a specification with predetermined controls, adding $B_r \cdot Post_t \cdot \mathbf{1}[f]$, where $B_r = (\log(\textit{pre size})_r, \textit{pre growth}_r)$ contains two pre-crisis RTO characteristics. The first is the logarithm of total two-wheeler registrations from April 2022 through November 2023. The second is the ratio of registrations in the late pre-period (February 2023–November 2023) to registrations in the early pre-period (April 2022–January 2023). Both variables are standardised within the estimation sample and are measured over the same predetermined period as exposure, so neither overlaps the event-study pre-trend window. The interaction $B_r \cdot Post_t \cdot \mathbf{1}[f]$ permits pre-shock size and growth to have different post-period associations with the two segments. It is not collinear with μ_{rt} because it varies by segment within an RTO-month; the unsegmented interaction $B_r \cdot Post_t$ is collinear with μ_{rt} and is therefore omitted. As a more flexible check, we interact B_r separately with each calendar month and segment indicator, $B_r \cdot \mathbf{1}[t = \tau] \cdot \mathbf{1}[f]$ for every $\tau \neq -1$, allowing the segment-specific loading on pre-shock size and growth to vary month by month. Standard errors are two-way clustered by RTO and state $\times$ month. A negative post-period β_τ indicates that non-Ola electric registrations weakened relative to ICE registrations as pre-shock Ola exposure increased.

Identifying assumption. The design does not require the absence of national shocks after September 2024: segment-by-month fixed effects absorb national changes that affect electric and ICE two-wheelers differently. A causal interpretation instead requires that, conditional on the fixed effects and predetermined controls, no other contemporaneous shock changed non-Ola electric registrations relative to ICE registrations in proportion to pre-shock Ola exposure. Potential violations include an unrelated contraction in non-Ola EV supply in high-Ola markets, state-specific policy changes, or administrative frictions whose effects were systematically larger in those markets. For example, PM E-DRIVE introduced an Aadhaar-authenticated e-voucher generated at the point of sale (Ministry of Heavy Industries, 2024b). Its nationwide effect is absorbed by segment-by-month fixed effects, but differential local implementation would not be. We assess these concerns using the event-study pre-trends, region- and state-specific segment-by-month effects, and the comparison with four-wheeler EVs.

Design 2: synthetic difference-in-differences. The second design provides a complementary counterfactual that does not use ICE registrations as a benchmark. It asks how electric two-wheeler registrations in markets with high pre-crisis Ola exposure would have evolved after September 2024 had they continued to follow the path of comparable lower-exposure markets. We classify the 221 RTOs in the top quartile of $\textit{Ola Exposure}_r$ as the high-exposure group. The remain-

ing 665 RTOs form the pool from which the comparison group is constructed. The top-quartile cutoff reflects the concentration of Ola's pre-crisis presence in the upper tail of the exposure distribution.

Synthetic difference-in-differences constructs this comparison using the pre-crisis outcome data (Arkhangelsky et al., 2021). First, it gives more weight to lower-exposure RTOs whose pre-crisis electric-registration paths most closely resemble the average path of the high-exposure group. These RTO weights, denoted $\hat{\omega}_i$, determine the composition of the synthetic comparison group. Second, it gives more weight to the pre-crisis months that provide the most informative baseline for comparing that synthetic group with the post-crisis period. These time weights, denoted $\hat{\lambda}_t$, determine how the pre-crisis difference between the two groups is summarized. The estimator then compares the pre-to-post change in the high-exposure group with the corresponding change in its weighted comparison group. The resulting average treatment effect on the treated (ATT) is therefore the average post-crisis departure of high-exposure RTOs from their synthetic counterfactual, after accounting for any average difference between the two groups before the crisis. A negative ATT indicates that registrations in high-exposure markets fell below the path implied by comparable lower-exposure markets.

The pre-crisis period is December 2023–August 2024, and the post-crisis period is September 2024–August 2025. We estimate the model separately for two outcomes: $\log(1+\text{non-Ola electric registrations})$ and $\log(1 + \text{all high-speed electric registrations})$. Each outcome receives its own RTO and time weights, so the all-electric estimate is a separate category-level comparison rather than a mechanical sum of the non-Ola estimate and Ola's own decline. A causal interpretation requires that, absent the crisis, the weighted high- and lower-exposure groups would have maintained their pre-crisis relationship after September 2024.

We use placebo-based inference with $1{,}000$ replications. Appendix A.3 reports pre-treatment fit, weight concentration, and placebo distributions.

3.3 Results

Static triple-difference estimates. The static results point to a negative exposure gradient. After September 2024, non-Ola electric registrations fell further relative to ICE registrations in RTOs with greater pre-crisis Ola exposure. Table 1 summarizes the average post-crisis effect. Column 1 reports the baseline fixed-effects model; column 2 additionally conditions on predetermined measures of pre-crisis market size and growth; and column 3 permits their associations to vary by month. We use column 2 as the preferred specification, which accounts for observable differences in market scale and growth while avoiding the additional parameterization required in column 3.

Across all three columns, the exposure gradient is negative and statistically significant. The coefficient is -0.065 in the baseline model and -0.118 in the preferred specification (both $p < 0.01$). Its increase in absolute value after accounting for pre-crisis market size and growth suggests that these differences attenuate, rather than drive, the negative gradient. Allowing their associations to vary by month leaves the coefficient unchanged at -0.118. Thus, the preferred result is not

Table 1: Static triple-difference estimates: non-Ola electric versus ICE two-wheelers

	No controls	Size/growth controls	Month-specific controls
Ola exp. × Post × Non-Ola	-0.065***	-0.118***	-0.118***
	(0.013)	(0.021)	(0.020)
Observations	37,212	37,212	37,212
Adjusted R-squared	0.975	0.975	0.975

Notes: The outcome is $\log(\textit{registrations}+1)$ at the RTO × segment × month level for the segments {non-Ola electric, ICE two-wheelers}. The sample contains 886 size-filtered RTOs observed from December 2023 through August 2025. The reported coefficient is on $\textit{Ola Exposure}_r \times \textit{Post}_t \times \mathbf{1}[f = \text{non-Ola electric}]$, where $\textit{Ola Exposure}_r = \log(1+\text{cum Ola}_r)$ is measured over April 2022–November 2023. All columns estimate the static analogue of Equation (3.2) with RTO × segment, RTO × month, and segment × month fixed effects. "No controls" includes only the triple interaction. "Size/growth controls" additionally allows predetermined RTO size and growth to have segment-specific post-period associations. "Month-specific controls" allows these segment-specific associations to vary by calendar month. Standard errors in parentheses are two-way clustered by RTO and state × month. $^{*}\,p<0.10$, $^{**}\,p<0.05$, $^{***}\,p<0.01$.

sensitive to whether these pre-crisis characteristics are permitted to have a common or month-specific post-crisis adjustment.

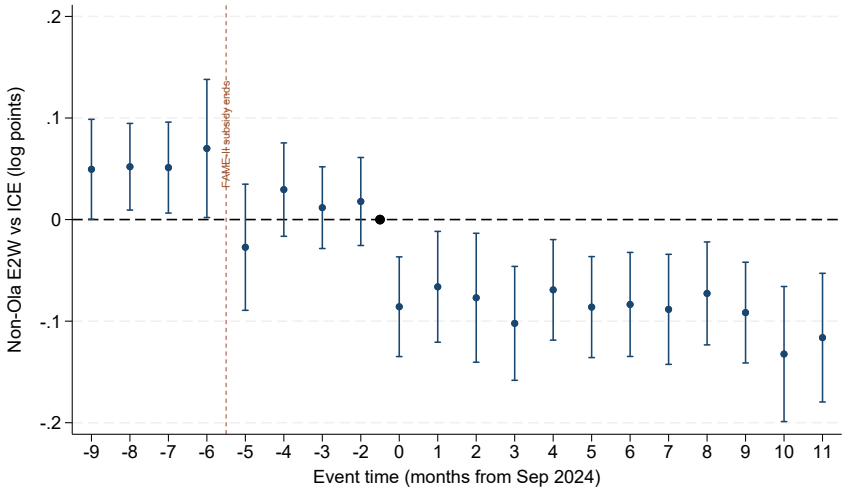
The implied difference across the exposure distribution is substantial. In column 2, a one-log-unit increase in pre-crisis Ola exposure—roughly a 2.7-fold increase in cumulative Ola registrations—corresponds to a 0.118 log-point decline in non-Ola electric registrations relative to ICE registrations. Exposure differs by 3.55 log units between the bottom and top quartiles, from 3.22 to 6.77 (Table A-5). Applying the preferred coefficient to this difference implies an approximately 34% relative shortfall in the top quartile compared with the bottom quartile.

Ola registrations had already begun to decline in July and August 2024, raising the concern that these months may not provide a clean pre-crisis benchmark. Dropping them yields a similar, slightly larger coefficient of -0.136 (Appendix A.9).

Event-study triple-difference. Figure 4 plots the results from event study specification in equation 3.2. The coefficient is negative for the treatment period starting September 2024 and remains negative throughout the following year.

The coefficients in the event study are significantly above 0 from December 2023 through March 2024, and then close to zero for the remaining pre-treatment period. This is due to the transition from a higher subsidy FAME-II regime which ended in March 2024 (Section 2). Reassuringly, the coefficient falls when the lower subsidy takes effect in April and remains close to the August reference level from May onward.

Figure 4: Event-study triple-difference: non-Ola electric versus ICE two-wheelers



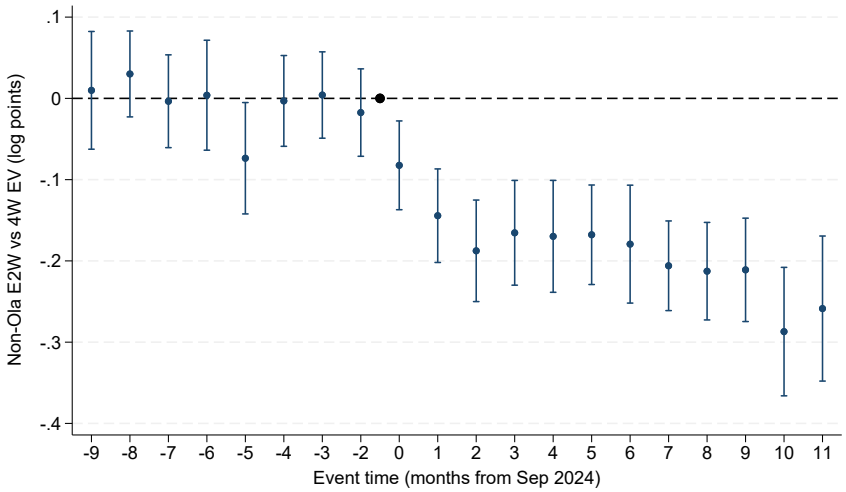
Notes: Estimated coefficients $\hat{\beta}_\tau$ from Equation (3.2) on *Ola Exposure*$_r$ $\times$ $\mathbf{1}[t - \text{Sep '24} = \tau] \times \mathbf{1}[f =$ non-Ola electric]. The specification includes RTO $\times$ segment, RTO $\times$ month, and segment $\times$ month fixed effects and the segment-specific controls used in the "Size/growth controls" column of Table 1. August 2024 ($\tau = -1$), shown by the black diamond, is the omitted reference month. Error bars are 95% confidence intervals. The sample contains 886 RTOs observed from December 2023 through August 2025. Appendix A.9 reports the donut-window specification. The vertical dashed line marks the expiry of the FAME-II purchase subsidy (31 March 2024).

A within-electric comparison: four-wheeler EVs. The baseline triple-difference compares non-Ola electric two-wheelers with ICE two-wheelers. Because ICE vehicles are not electric, this comparison may retain broader pre-period dynamics in EV demand, including adoption growth, changes in the central purchase subsidy, and charging-network expansion. These dynamics are also concentrated in mature, high-penetration EV markets with high Ola exposure. A negative exposure gradient could therefore reflect differential EV-market trends rather than the reputational shock. To assess this possibility, we re-estimate Equation (3.2) using four-wheeler EVs instead of ICE two-wheelers as the comparison segment. Ola did not produce four-wheelers, so this within-electric comparison absorbs local determinants shared across EV segments without directly exposing the control segment to the Ola shock. Under an Ola-segment-specific spillover, non-Ola electric two-wheelers should weaken relative to four-wheeler EVs after the crisis, without a corresponding differential pre-trend.

The estimates are consistent with that prediction. After September 2024, non-Ola electric two-wheelers decline relative to four-wheeler EVs as Ola exposure increases. The static coefficient is -0.129 log points per log unit of exposure without controls and -0.184 with the $B_r \times Post$ controls (both $p < 0.01$). A Poisson count specification yields -0.074 ($p < 0.01$), indicating that the negative sign is not specific to the logarithmic transformation (Appendix A.12, Table A-14). In the event study (Figure 5), the eight pre-shock coefficients are close to zero, the differential emerges in September, and its magnitude increases through August 2025. Relative to the ICE comparison, differencing against another electric segment removes more of the pre-period EV-market variation.

This comparison improves the interpretation but is not a definitive placebo. Two- and four-wheeler EVs differ in buyers, prices, uses, and policy treatment; in particular, four-wheeler EVs were excluded from both EMPS and PM E-DRIVE. The control segment therefore cannot absorb every shock specific to electric two-wheelers. We therefore interpret the comparison as evidence against a generic local EV-demand explanation, not as conclusive identification of the mechanism.

Figure 5: Event study: non-Ola electric two-wheelers versus four-wheeler EVs



Notes: Event-study estimates $\hat{\beta}_\tau$ from Equation (3.2), replacing ICE two-wheelers with four-wheeler EVs as the comparison segment and including $B_r \times Post_t \times \mathbf{1}[f]$ controls. Coefficients are measured relative to August 2024. The outcome is $\log(Registrations + 1)$, and treatment intensity is pre-shock $Ola\ Exposure_r$. Error bars are 95% confidence intervals based on standard errors two-way clustered by RTO and state × month. A joint test does not reject that the eight pre-shock coefficients equal zero ($p = 0.14$). The sample contains 886 RTOs observed from December 2023 through August 2025. Appendix A.12 reports the construction and static estimates.

Synthetic difference-in-differences. Table 2 compares electric two-wheeler registrations in high-Ola-exposure RTOs with the path predicted by their synthetic comparison group. From September 2024 through August 2025, non-Ola electric registrations were 0.181 log points below this counterfactual, implying that these RTOs registered approximately 17% fewer non-Ola electric two-wheelers than they otherwise would have. This is a shortfall relative to the counterfactual path, not necessarily an absolute decline in registrations. When the outcome is expanded to include Ola, total electric two-wheeler registrations were approximately 12% below their counterfactual. This indicates that the decline in Ola registrations was not fully offset by growth among non-Ola manufacturers, leaving overall electric adoption weaker in the markets most exposed to Ola. The two estimates should not be combined mechanically because SDID constructs a separate synthetic comparison group for each outcome.

Figure 6 plots the treated and synthetic-control trajectories for the non-Ola and all-electric outcomes. Because treated RTOs are larger EV markets, the unadjusted trajectories need not coincide in levels. The relevant diagnostic is whether the weighted treated-synthetic difference is stable

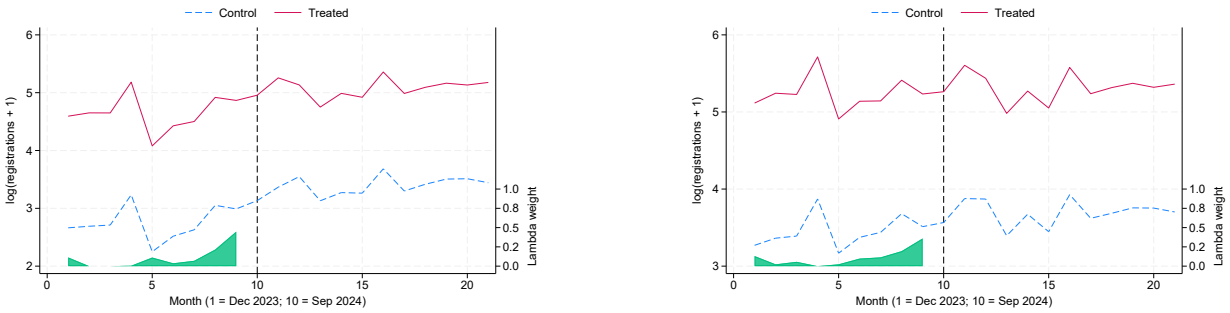
Table 2: Synthetic difference-in-differences estimates

	(1) Non-Ola electric 2W	(2) All electric 2W
ATT	-0.181***	-0.126***
	(0.030)	(0.023)
95% CI	[-0.241, -0.122]	[-0.171, -0.081]
Treated areas	221	221
Control areas	665	665
Months	21	21
Placebo reps	1,000	1,000

Synthetic difference-in-differences estimates following Arkhangelsky et al. (2021), with treatment beginning in September 2024. The sample covers December 2023–August 2025 (9 pre-treatment and 12 post-treatment months) without a donut exclusion. Outcomes are $\log(\textit{registrations}+1)$ at the RTO $\times$ month level. Treated RTOs (221) are in the nationwide top quartile of cumulative Ola registrations measured over April 2022–November 2023; the 665 RTOs in the lower three quartiles form the control pool. Standard errors in parentheses are obtained from 1,000 placebo reassignments. $^{*}\,p<0.10$, $^{**}\,p<0.05$, $^{***}\,p<0.01$.

before treatment. The divergence after September 2024, together with the placebo distribution and weight diagnostics in Appendix A.3, provides evidence consistent with the triple-difference results.

Figure 6: Synthetic difference-in-differences trajectories



(a) $\log(\text{non-Ola electric two-wheelers} + 1)$ (b) $\log(\text{all electric two-wheelers} + 1)$

Notes: The treated series (red, solid) represents the 221 RTOs in the nationwide top quartile of cumulative Ola registrations over April 2022–November 2023. The synthetic-control series (blue, dashed) is a weighted average of the 665 RTOs in the lower three quartiles, using unit weights $\hat{\omega}_i$ from Arkhangelsky et al. (2021). The month index is 1 = December 2023, 10 = September 2024 (the treatment month, marked by the dashed vertical line), and 21 = August 2025. Shaded mass indicates the estimated time weights $\hat{\lambda}_t$. Table 2 reports the average treatment effects and inference.

Levels decomposition. The triple-difference estimates show that non-Ola electric registrations weakened relative to ICE registrations, but they do not reveal which registration margin generated that change. Non-Ola electric registrations may have grown more slowly, ICE registrations may have increased, or both may have occurred. We therefore estimate separate RTO-level difference-in-differences specifications for each registration outcome.

$$y_{rt} = \alpha_r + \lambda_t + \beta \cdot (\textit{Ola Exposure}_r \cdot \textit{Post}_t) + B_r \cdot \gamma \cdot \textit{Post}_t + \varepsilon_{rt}. \tag{3.3}$$

Each model includes RTO and calendar-month fixed effects, predetermined controls $B_r \cdot \textit{Post}_t$, and standard errors two-way clustered by RTO and state $\times$ month. These controls are the same standardised size and growth covariates used in the triple-difference, without a segment interaction because each outcome is estimated separately. The five outcomes are log non-Ola E2W registrations, log ICE registrations, log total electric registrations, log total two-wheeler registrations, and the EV-to-ICE log ratio $\log[(\text{EV}+1)/(\text{ICE}+1)]$.

Table 3 reports the descriptive levels. In the top quartile of pre-shock Ola exposure, average monthly non-Ola E2W registrations rose from 172 to 243 per RTO between the pre- and post-periods; in the lower three quartiles, they rose from 26 to 46. Ola registrations moved in the opposite direction, declining from 106 to 56 in Q_4 and from 21 to 14 in Q_1–Q_3. ICE registrations increased in both groups. The principal descriptive difference is compositional: the EV share of two-wheeler registrations was nearly unchanged in high-exposure areas, moving from 11.2% to 11.3%, while it increased from 4.8% to 5.9% in lower-exposure areas.

Table 4 reports the continuous-treatment DiD estimates for each outcome. The non-Ola E2W coefficient is -0.100 ($p < 0.01$). Conditional on RTO and calendar-month fixed effects and predetermined size and growth controls, a one-log-unit increase in pre-shock Ola exposure is therefore associated with an approximately 10% post-period shortfall in non-Ola E2W registrations. The ICE coefficient is small and positive (0.017), while the coefficient for total two-wheeler registrations is 0.013; neither is statistically significant. These estimates show no detectable differential increase in ICE registrations or change in total two-wheeler registrations.

The clearest negative coefficients are for total EV registrations (-0.090, significant at 1%) and the EV-to-ICE log ratio (-0.107, significant at 1%). These estimates indicate that electric registrations grew less in high-exposure areas and that the EV-to-ICE ratio followed a lower path than the model's counterfactual.

Table 3: Per-outcome decomposition: descriptive levels

	High exposure (Q_4)			Lower exposure (Q_1–Q_3)			
	Pre-crisis	Post-crisis	Change	Pre-crisis	Post-crisis	Change	DiD
Ola registrations	106.2	55.6	-50.6	20.9	14.4	-6.5	-44.1
Non-Ola E2W registrations	172.3	242.7	70.4	26.1	46.0	19.9	50.4
ICE registrations	2,466.8	2,706.1	239.4	1,150.5	1,215.0	64.5	174.8
Total 2W registrations	2,745.3	3,004.4	259.1	1,197.4	1,275.4	77.9	181.2
EV share of 2W (%)	11.21	11.29	0.08	4.79	5.87	1.08	-1.00

The sample contains 886 size-filtered RTOs. Q_4 is the top quartile of $\log(1+\textit{cum Ola}_r)$ measured over April 2022–November 2023; Q_1–Q_3 comprise the lower three quartiles. Entries are average monthly registrations per RTO. The pre-period is December 2023–August 2024, and the post-period is September 2024–August 2025. "DiD" is the change in Q_4 minus the change in Q_1–Q_3. "EV share of 2W" is the average RTO-month percentage share within each exposure group and period.

Table 4: Per-outcome continuous-treatment difference-in-differences estimates

	Non-Ola electric 2W	ICE 2W	All electric 2W	All 2W	Electric/ICE ratio
Ola exp. × Post	-0.100***	0.017	-0.090***	0.013	-0.107***
	(0.019)	(0.012)	(0.014)	(0.012)	(0.017)
Observations	18,606	18,606	18,606	18,606	18,606
Adj. R-sq	0.893	0.925	0.903	0.928	0.828

Notes: Each column estimates Equation (3.3) separately at the RTO × month level with RTO and calendar-month fixed effects. Outcomes are log non-Ola E2W registrations, log ICE registrations, log total electric registrations, log total two-wheeler registrations, and the EV-to-ICE log ratio $\log[(\text{EV}+1)/(\text{ICE}+1)]$. Every specification includes standardised pre-shock size and growth interacted with $\textit{Post}_t$. Standard errors in parentheses are two-way clustered by RTO and state × month. The sample window is December 2023–August 2025. $^{*}\,p<0.10$, $^{**}\,p<0.05$, $^{***}\,p<0.01$.

A separate count-based analysis in Appendix A.13 puts the scale of the shortfall into perspective. Across the 221 most exposed RTOs, approximately 644,000 non-Ola electric two-wheelers were registered from September 2024 through August 2025, compared with an estimated 756,000 under the national counterfactual. This shortfall of 113,000 represents about 15% of expected registrations. Allowing each state to follow its own segment-specific monthly trajectory reduces the estimated shortfall to approximately 59,000 registrations.

Whether these purchases shifted to ICE vehicles or were postponed remains unresolved. Under the national counterfactual, an increase of only about 1.6% in ICE registrations would offset the entire non-Ola electric shortfall. The confidence interval for the ICE response readily accommodates an increase of that size. The estimates therefore establish weaker electric adoption without determining the destination of the missing purchases.

3.4 Robustness

This section evaluates the sensitivity of the baseline estimates to four sets of choices: the measurement of exposure and outcomes, the inclusion of more restrictive geographic fixed effects, the functional form of the exposure-response relationship, and the length and definition of the post-treatment period. A final exercise asks whether the gradient is specific to Ola rather than to the geography of large electric two-wheeler incumbents. For the SDID estimates, Appendix A.3 verifies two conditions: the unit weights spread over several hundred effective control RTOs, so the synthetic comparison is not driven by a small set of look-alike markets, and the estimated effect lies well below the distribution of placebo effects from random treatment assignment.

Measurement of exposure and outcomes. To verify that our empirical baseline is not an artifact of functional-form choices, we explicitly test how results change under alternate transformations of treatment and outcome variables. In skewed count data, standard practice relies on log-like transformations—specifically $\log(1 + \text{cum Ola}_r)$ for exposure and $\log(Y + 1)$ for registrations. However, these transformations introduce two potential econometric vulnerabilities: they artificially compress the distance between high- and low-exposure markets, and they impose specific implicit weights on zero-valued outcome cells. As Chen and Roth (2024) formalize, when zero counts are present, log-like transformations can make estimated coefficients sensitive to the units of measurement by altering the relative weight placed on the extensive versus intensive margins.

We therefore evaluate the sensitivity of our findings by systematically altering these transformation choices while holding the rest of the research design fixed. In Appendix Table A-1, we replace the baseline exposure metric with an inverse hyperbolic sine transformation, $\sinh^{-1}(\text{cum Ola}_r)$, which smoothly accommodates zero values. In Appendix Table A-2, we maintain the baseline exposure metric but apply $\sinh^{-1}(Y)$ to the outcome variable. Under our primary specification with $B_r \times \textit{Post}$ controls, the estimated spillover coefficient yields -0.114 under the $\sinh^{-1}$ exposure and -0.141 under the $\sinh^{-1}$ outcome. Both point estimates remain statistically significant at the 1% level and closely track our baseline point estimate of -0.118.

Finally, to directly test whether extensive-margin shifts contaminate our results, Appendix A.10 examines the distribution of zero-valued cells. Zero counts are extremely rare within our size-filtered analytical sample (Table A-12), and the proportion of zero-registration periods in exposed areas remains static across the shock (Table A-13). Taken together, these diagnostics confirm that our estimates capture genuine adjustments along the intensive margin rather than mathematical artifacts driven by scale transformations or the treatment of zero outcomes.

Geographic confounding. A central challenge to causal identification is spatial confounding. Because pre-shock Ola exposure is spatially clustered (Figure 3), an unadjusted comparison risks confounding the shock's true impact with broader, region-specific trajectories in electric vehicle adoption. To isolate local exposure effects from macro-geographic trends, we progressively saturate the model with high-dimensional fixed effects that absorb unobserved spatial heterogeneity.

We first incorporate region $\times$ segment $\times$ month fixed effects in Appendix Table A-6. This flexible structure allows each broad geographic region to follow an independent, time-varying trajectory for every vehicle segment. Upon absorbing these regional trends, the point estimate moderates slightly from -0.118 to -0.091 while retaining significance at the 1% level. This demonstrates that the vast majority of the estimated effect is identified from variation across Regional Transport Offices (RTOs) located within the exact same geographic zone.

To implement an even more demanding test, Appendix Table A-7 incorporates state $\times$ segment $\times$ month fixed effects. This specification absorbs all state-level, segment-specific monthly shocks, identifying the parameter exclusively from comparisons among RTOs within the same state, segment, and calendar month. Under this specification, the linear point estimate declines to -0.047 ($p \approx 0.06$). This attenuation reflects two underlying factors: the removal of meaningful between-state variation and the structural difficulty of fitting a constant linear slope within narrow, geographically homogenous state sub-samples. To test whether local non-linearities drive the response, Appendix Table A-8 compares high-exposure RTOs (top quartile and top quintile) against lower-exposure RTOs within the same state. These within-state binary comparisons yield robust, statistically significant estimates of -0.196 and -0.209 ($p < 0.01$). This confirms that local exposure generates strong spillovers even when strictly evaluating within-state variation.

Functional form of the dose-response. Our baseline specification imposes a constant linear elasticity with respect to log exposure. If consumer responses are non-linear—for instance, if market spillovers manifest primarily once exposure crosses a critical threshold—a continuous linear term will understate the effect in highly exposed markets and overstate it elsewhere. To evaluate the dose-response relationship without imposing structural functional-form constraints, we re-estimate the model replacing continuous exposure with indicators for exposure quintiles (Appendix Table A-9).

The non-parametric estimates reveal that the adverse spillover is heavily concentrated in the upper tail of the exposure distribution. Relative to the lowest quintile, the estimated differential is -0.115 in the fourth quintile and reaches -0.456 in the fifth quintile. Crucially, high-exposure RTOs in these upper quintiles are geographically dispersed across multiple states, confirming that this high-exposure penalty reflects a widespread economic pattern rather than idiosyncratic dynamics within a single state.

The transition months. A practical complication in identifying the precise timing of the shock is that Ola's registration volumes began declining in July and August 2024—two months prior to the widely reported September events (Figure 2). If prospective EV buyers in exposed markets began altering their purchasing behavior during these transition months, incorporating July and August 2024 into the pre-period would contaminate baseline levels and attenuate our post-shock estimates.

To eliminate this potential pre-treatment contamination, we estimate a "donut" specification

that explicitly drops July and August 2024 from the sample. By removing these transition months, identification rests entirely on periods that are unambiguously prior to or following the shock. As shown in Appendix Table A-11, the resulting point estimate of -0.136 is slightly larger in magnitude than the baseline estimate of -0.118. This confirms that early buyer responses during the transition months introduced mild downward attenuation in our baseline model, and that the clean post-shock contrast is slightly stronger than initially reported.

Persistence. Understanding the temporal path of the spillover is critical for determining whether the shock caused a temporary purchasing delay or a persistent shift in market demand. If the disruption were merely a short-term friction, deferred purchases would resume in subsequent periods, causing the estimated negative gradient to attenuate over time. To test for long-run persistence, Appendix Table A-10 divides the post-period into two distinct time horizons: an initial one-year post-shock block (September 2024–August 2025) and a longer-run block (September 2025–March 2026), estimating separate coefficients for each window.

The point estimates across these two horizons are statistically indistinguishable: -0.118 for the first year and -0.111 for the second ($p = 0.53$). This demonstrates that the negative exposure gradient neither fades nor deepens through early 2026. While longer time horizons naturally introduce potential confounding events—leading us to interpret the second-year estimate as descriptive rather than strictly causal—the absence of mean reversion indicates that the shock created a durable adjustment in relative market adoption rather than a transient purchasing pause.

Placebo exposure. A final identification concern is that our exposure variable might capture broader spatial characteristics inherent to major electric two-wheeler incumbents rather than the brand-specific reputational shock suffered by Ola. To test whether general incumbent geography drives our findings, we construct a placebo exposure metric based on TVS, the second-largest electric two-wheeler manufacturer during our exposure window. TVS shared a similar spatial distribution with Ola during this period but experienced no comparable reputational crisis.

We construct TVS exposure analogously to Ola exposure—$\log(1 + \text{cum TVS}_r)$ calculated over April 2022–November 2023—and re-estimate our triple-difference specification. To ensure that neither brand's own sales mechanically affect the outcome, the dependent variable in both regressions is defined as the log count of electric two-wheelers excluding both Ola and TVS, differenced against ICE registrations. If spatial clustering of major EV incumbents were driving the effect, both exposure measures should yield similar post-shock trajectories.

Instead, the post-shock dynamics diverge significantly in their persistence (Appendix A.11, Figure A-8). While both gradients turn briefly negative after September 2024—reflecting shared geographic exposure to EV adoption trends—the TVS gradient is shallower and rapidly reverts toward zero within a few months. In contrast, the Ola exposure gradient stabilizes near -0.06 log points and remains persistently negative through August 2025 (with overall static coefficients of -0.077 for Ola versus -0.055 for TVS). Although overlapping confidence intervals mean this

contrast should be interpreted as suggestive rather than definitive, the distinct persistence profile strongly supports the hypothesis that the sustained negative spillovers were driven specifically by Ola's reputational shock.

4 Mechanism: service-network congestion

In order to demonstrate that trust failures drive our results, we must isolate a concrete transmission channel: consumers' direct observation of Ola's failing service infrastructure. In January 2024, Ola operated just 432 dedicated service centres nationwide; 66% of served districts contained a single facility, the median district sat 36 km from the nearest centre, and owners in the median district queued at sites serving roughly 630 scooters. If observable service breakdowns transmitted the shock, post-September 2024 non-Ola electric registrations should exhibit greater attrition in markets with higher workshop congestion, conditional on Ola's local installed base.

We reconstruct the network from Ola's site listings as captured by the Internet Archive on 3 January 2024 (Ola Electric, 2024). 98% of centres carry verified coordinates, and the snapshot predates both the crisis and Ola's subsequent service expansion. Each Census-2011 district's predetermined Ola fleet is

$$Fleet_d = \sum_{t=\text{Apr 2022}}^{\text{Nov 2023}} Ola_{dt}, \tag{4.1}$$

where Ola_{dt} aggregates Ola_{rt} over the district's RTOs; the window is the exposure window. Let S_d denote the workshop sites district d's owners use: the centres located in d when the district contains any, and the single nearest centre otherwise. Fleets queue under this rule, so a site's queue and the district's *queue load* are

$$Q_s = \sum_{d:\, s \in S_d} \frac{Fleet_d}{|S_d|}, \qquad Load_d = \frac{1}{|S_d|} \sum_{s \in S_d} Q_s. \tag{4.2}$$

The regressor is $z(\log Load_d)$, standardised after trimming at the 5th and 95th percentiles of the district distribution. Each RTO inherits the value of its district (787 RTOs), so the identifying variation is at the district level.

The event study augments Equation (3.2) with the queue-load interactions:

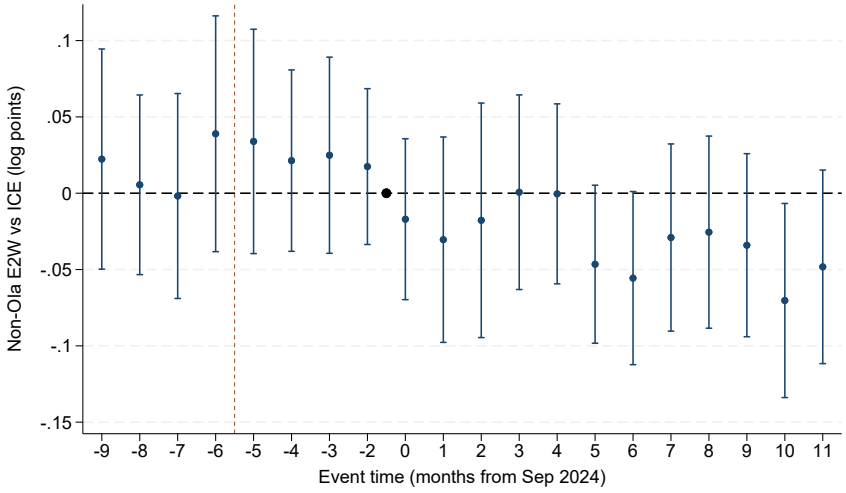
$$\begin{aligned}\log(Registrations_{rft} + 1) = \alpha_{rf} + \mu_{rt} + \delta_{ft} + \sum_{\tau \neq -1} \theta_\tau (z(\log Load)_r \cdot \mathbf{1}[t - \text{Sep '24} = \tau] \cdot \mathbf{1}[f = \text{non-Ola}]) \\ + \sum_{\tau \neq -1} \beta_\tau (Ola\ Exposure_r \cdot \mathbf{1}[t - \text{Sep '24} = \tau] \cdot \mathbf{1}[f = \text{non-Ola}]) + \varepsilon_{rft},\end{aligned} \tag{4.3}$$

with the $B_r \times Post \times \mathbf{1}[f]$ controls, two-way clustering by RTO and state × month, and August 2024 the omitted month. The static version replaces the event-time indicators with $Post_t$.

Figure 7 presents the event-study estimates. The eight pre-shock leads are jointly indistin-

guishable from zero ($p = 0.96$). Following the shock, the queue-load differential remains near zero from September through January, turns negative in February–March 2025 (-0.047 and -0.056), and reaches its maximum effect size in July 2025 (-0.070, $t = -2.2$). Table 5 reports the static specifications: a one-standard-deviation increase in queue load reduces non-Ola registrations by -0.049 without geographic controls ($t = -2.6$), -0.043 under region × segment × month fixed effects ($t = -2.2$), and -0.034 under state × segment × month fixed effects ($t = -2.0$).

Figure 7: Queue load at Ola service centres and non-Ola registrations



Notes: Event-study coefficients on $z(\textit{queue load})_r \times \mathbf{1}[t - \text{Sep '24} = \tau] \times \mathbf{1}[f = \text{non-Ola}]$, estimated jointly with the exposure event-time interactions and the $B_r \times \textit{Post} \times \mathbf{1}[f]$ controls, with RTO × segment, RTO × month, and segment × month fixed effects. August 2024 (black dot) is the omitted month. Error bars are 95% confidence intervals based on standard errors two-way clustered by RTO and state × month. Sample: 787 RTOs, December 2023–August 2025. The vertical dashed line marks the expiry of the FAME-II purchase subsidy (31 March 2024).

Table 5: Queue load and the post-crisis non-Ola differential

	No geographic FE	Region×Seg×Mo	State×Seg×Mo
z(Queue load) × Post × Non-Ola	-0.049**	-0.043**	-0.033**
	(0.019)	(0.019)	(0.017)
Observations	33,054	33,054	32,928

Static version of the specification in Figure 7, with the event-time indicators replaced by $\textit{Post}_t$. Every column includes the $\textit{Ola Exposure}_r \times \textit{Post}_t \times \mathbf{1}[f = \text{non-Ola}]$ interaction and the $B_r \times \textit{Post} \times \mathbf{1}[f]$ controls (not shown). Columns add region × segment × month and state × segment × month fixed effects to the baseline three-way structure, as for the main outcome. Sample and two-way clustering by RTO and state × month as in Figure 7. $^{*}\, p < 0.10$, $^{**}\, p < 0.05$, $^{***}\, p < 0.01$.

In sum, these results suggest that service-network congestion may have served as a transmission channel for trust degradation. Severe workshop queues could have exposed prospective

buyers to visible operational failures. This exposure might have eroded confidence across the broader EV market.

5 Conclusion

The transition to cleaner technologies depends partly on whether consumers believe that unfamiliar products will work reliably and remain serviceable after purchase. In emerging markets, where durable goods represent substantial household investments, confidence in these promises can shape the willingness to adopt. Yet consumers often learn about a new technology through their experience with a small number of prominent producers. The performance of those firms can therefore have consequences beyond their own customers and market shares: it can influence confidence in the technology and the pace of its diffusion. This paper examines that connection between firm-level service reliability and the broader process of decarbonization.

The 2024 service crisis at Ola Electric provides evidence that these consequences can extend to competing producers. Using geographic variation in Ola's pre-crisis installed base, we find that non-Ola electric two-wheeler registrations weakened more in Indian markets with greater exposure to Ola. The result appears both when benchmarking electric registrations against ICE registrations and when comparing highly exposed markets with a synthetic comparison of lower-exposure markets. In the most exposed quartile, non-Ola registrations were approximately 17% below their synthetic counterfactual during the following year. Electric registrations continued to grow, but the crisis was associated with slower expansion of the category beyond the affected firm. Additional weakness in markets with greater estimated pressure on Ola's service network links this pattern to the local infrastructure supporting the technology.

These findings connect the reputation of individual producers to the adoption of emerging technologies. When buyers interpret one producer's failures as informative about the wider category, competing firms may bear some of the consequences of service decisions they do not control. Reliable after-sales support can thus have value beyond the firm providing it, while inadequate support can discourage adoption beyond that firm's customer base. This interdependence is particularly consequential early in a technology's diffusion, when consumers have limited experience on which to base their judgments and prominent producers play a large role in shaping expectations.

For decarbonization policy, the implication is that expanding sales and sustaining adoption are closely connected to the capacity to support products already in use. Purchase incentives and charging infrastructure address important barriers to electrification, while repair capacity, dependable after-sales service, and credible consumer protection help sustain confidence as the installed fleet grows. Where scooters and motorcycles account for a large share of personal mobility, failures in this supporting infrastructure can have implications for a substantial part of the transport transition. The broader lesson is that the firms bringing a clean technology to market also help establish its credibility.

References

Acemoglu, Daron, David Autor, David Dorn, Gordon H Hanson, and Brendan Price, "Import Competition and the Great US Employment Sag of the 2000s," *Journal of Labor Economics*, 2016, *34* (S1), S141–S198. 1

Akerlof, George A., "The Market for "Lemons": Quality Uncertainty and the Market Mechanism," *The Quarterly Journal of Economics*, 1970, *84* (3), 488–500. 1

Arkhangelsky, Dmitry, Susan Athey, David A Hirshberg, Guido W Imbens, and Stefan Wager, "Synthetic difference-in-differences," *American Economic Review*, 2021, *111* (12), 4088–4118. 1, 3.2

Autocar Professional, "Electric 2W sales jump 40% in September; Bajaj Chetak outsells TVS iQube, Ola share falls to 27%," https://www.autocarpro.in/analysis-sales/electric-2w-sales-jump-40-in-september-bajaj-chetak-outsells-tvs-iqube-ola-share-falls-to-27- 2024. Attributes soft September retail partly to reduced pre-deadline urgency after the EMPS extension into PM E-DRIVE and partly to the Pitru Paksh fortnight. 2

_ , "Govt launches Rs. 10,900 crore PM E-DRIVE scheme to replace FAME-II," https://www.autocarpro.in/news/govt-launches-rs-10900-crore-pm-e-drive-scheme-to-replace-fame-2-122528 2024. Two-year, Rs. 10,900 crore scheme covering electric two- and three-wheelers, buses, trucks, ambulances, and charging infrastructure. 2

_ , "PM E-DRIVE comes into effect tomorrow; 2W and 3W subsidies to halve from April," https://www.autocarpro.in/news/pm-e-drive-comes-into-effect-tomorrow-2w-and-3w-subsidies-to-halve-from-april-122817 2024. Electric two-wheeler incentive held at Rs. 5,000 per kWh (cap Rs. 10,000) for the first year of PM E-DRIVE, the same as EMPS, then halved to Rs. 2,500 per kWh (cap Rs. 5,000) from April 2025. 2, A.12

Autor, David H, David Dorn, and Gordon H Hanson, "The China Syndrome: Local Labor Market Effects of Import Competition in the United States," *American Economic Review*, 2013, *103* (6), 2121–68. 1

Bachmann, Rüdiger, Gabriel Ehrlich, Ying Fan, Dimitrije Ruzic, and Benjamin Leard, "Firms and Collective Reputation: A Study of the Volkswagen Emissions Scandal," *Journal of the European Economic Association*, 2023, *21* (2), 484–525. 1

Bai, Jie, Ludovica Gazze, and Yukun Wang, "Collective Reputation in Trade: Evidence from the Chinese Dairy Industry," *The Review of Economics and Statistics*, 2022, *104* (6), 1121–1137. 1

Bhat, Furqan A. and Ashish Verma, "Electric Two-Wheeler Adoption in India – A Discrete Choice Analysis of Motivators and Barriers Affecting the Potential Electric Two-Wheeler Buyers," *Transport Policy*, 2024, *152*, 118–131. 1

Bond, Eric W., "A Direct Test of the "Lemons" Model: The Market for Used Pickup Trucks," *The American Economic Review*, 1982, *72* (4), 836–840. 1

Borah, Abhishek and Gerard J. Tellis, "Halo (Spillover) Effects in Social Media: Do Product Recalls of One Brand Hurt or Help Rival Brands?," *Journal of Marketing Research*, 2016, *53* (2), 143–160. 1, 1

Briceno-Garmendia, Cecilia, Wenxin Qiao, and Vivien Foster, "The Economics of Electric Vehicles for Passenger Transportation," Technical Report, World Bank, Mobility and Transport Connectivity Series 2022. 1, 1

Business Standard, "Over 10k complaints filed against Ola Electric; CCPA sends notice," https://www.business-standard.com/companies/news/over-10k-complaints-filed-against-ola-electric-ccpa-sends-notice-124101100817_1.html 2024. Central Consumer Protection Authority show-cause notice, 7 October 2024, over 10,644 National Consumer Helpline complaints (September 2023–August 2024). 1, 2

Cabral, Luís and Ali Hortaçsu, "The dynamics of seller reputation: Evidence from eBay," *The Journal of Industrial Economics*, 2010, *58* (1), 54–78. 1

Chakraborty, Rahul and Sujoy Chakravarty, "Factors Affecting Acceptance of Electric Two-Wheelers in India: A Discrete Choice Survey," *Transport Policy*, 2023, *132*, 27–41. 1

Chen, Jiafeng and Jonathan Roth, "Logs with Zeros? Some Problems and Solutions," *The Quarterly Journal of Economics*, 2024, *139* (2), 891–936. 3.4, A.10

Cleeren, Kathleen, Marnik G. Dekimpe, and Kristiaan Helsen, "Weathering Product-Harm Crises," *Journal of the Academy of Marketing Science*, 2008, *36* (2), 262–270. 1

Dawar, Niraj and Madan M. Pillutla, "Impact of Product-Harm Crises on Brand Equity: The Moderating Role of Consumer Expectations," *Journal of Marketing Research*, 2000, *37* (2), 215–226. 1

Egbue, Ona and Suzanna Long, "Barriers to Widespread Adoption of Electric Vehicles: An Analysis of Consumer Attitudes and Perceptions," *Energy Policy*, 2012, *48*, 717–729. 1

Freedman, Seth, Melissa S. Kearney, and Mara Lederman, "Product Recalls, Imperfect Information, and Spillover Effects: Lessons from the Consumer Response to the 2007 Toy Recalls," *The Review of Economics and Statistics*, 2012, *94* (2), 499–516. 1, 1

Gallagher, Kelly Sims and Erich Muehlegger, "Giving Green to Get Green? Incentives and Consumer Adoption of Hybrid Vehicle Technology," *Journal of Environmental Economics and Management*, 2011, *61* (1), 1–15. 1

Genesove, David, "Adverse Selection in the Wholesale Used Car Market," *Journal of Political Economy*, 1993, *101* (4), 644–665. 1

Heerde, Harald J. Van, Kristiaan Helsen, and Marnik G. Dekimpe, "The Impact of a Product-Harm Crisis on Marketing Effectiveness," *Marketing Science*, 2007, *26* (2), 230–245. 1, 1

Hendel, Igal and Alessandro Lizzeri, "Adverse Selection in Durable Goods Markets," *American Economic Review*, 1999, *89* (5), 1097–1115. 1

Holland, Stephen P., Erin T. Mansur, Nicholas Z. Muller, and Andrew J. Yates, "Are There Environmental Benefits from Driving Electric Vehicles? The Importance of Local Factors," *American Economic Review*, 2016, *106* (12), 3700–3729. 1

Imbens, Guido W and Donald B Rubin, *Causal Inference for Statistics, Social, and Biomedical Sciences*, Cambridge University Press, 2015. A.4

Jarrell, Gregg and Sam Peltzman, "The Impact of Product Recalls on the Wealth of Sellers," *Journal of Political Economy*, 1985, *93* (3), 512–536. 1, 1

Jin, Ginger Zhe and Phillip Leslie, "The Effect of Information on Product Quality: Evidence from Restaurant Hygiene Grade Cards," *The Quarterly Journal of Economics*, 2003, *118* (2), 409–451. 1

Lewis, Gregory, "Asymmetric Information, Adverse Selection and Online Disclosure: The Case of eBay Motors," *American Economic Review*, 2011, *101* (4), 1535–1546. 1

Li, Shanjun, Binglin Wang, Muxi Yang, and Fan Zhang, "The Global Diffusion of Electric Vehicles: Lessons from the First Decade," Technical Report, World Bank Policy Research Working Paper No. 9882 2021. 1, 1

_ **, Lang Tong, Jianwei Xing, and Yiyi Zhou**, "The market for electric vehicles: Indirect network effects and policy design," *Journal of the Association of Environmental and Resource Economists*, 2017, *4* (1), 89–133. 1, 1

Ministry of Heavy Industries, "Faster Adoption and Manufacturing of Electric Vehicles in India, Phase II (FAME II)," Government of India. https://heavyindustries.gov.in/ 2019. Operative 1 April 2019 to 31 March 2024. Electric two-wheeler demand incentive reduced from Rs. 15,000 to Rs. 10,000 per kWh effective 1 June 2023. 2

_ , "Electric Mobility Promotion Scheme (EMPS) 2024," Government of India. https://emps.heavyindustries.gov.in/ 2024. Notified vide Gazette of India S.O. 1334(E), 13 March 2024; operative 1 April 2024, initially to 31 July 2024 and extended to 30 September 2024. Electric two-wheeler demand incentive Rs. 5,000 per kWh, capped at Rs. 10,000 per vehicle. 2, A.12

_ , "PM E-DRIVE Scheme: Operational Guidelines," Government of India. https://heavyindustries.gov.in/sites/default/files/2025-07/operatioal-guidelines-dt-30-09-2024-for-p-e-drive.pdf 2024. Dated 30 September 2024. The demand incentive is disbursed through an Aadhaar-authenticated e-voucher generated at the point of sale and tied to vehicle registration. 3.2

_ , "PM Electric Drive Revolution in Innovative Vehicle Enhancement (PM E-DRIVE) Scheme," Government of India. https://pmedrive.heavyindustries.gov.in/ 2024. Notified vide Gazette of India S.O. 4259(E), 29 September 2024; operative 1 October 2024 to 31 March 2026, outlay Rs. 10,900 crore. Subsumes EMPS 2024; the EMPS electric two-wheeler incentive rate carried into the first year. 2, A.12

Ministry of Road Transport and Highways, "VAHAN National Vehicle Registry: Vahan Dashboard," Government of India, National Informatics Centre. https://analytics.parivahan.gov.in/analytics/publicdashboard/vahan 2026. Administrative new-vehicle registration records by Regional Transport Office, month, maker, vehicle class, and fuel type. The registration data used in this paper span April 2022 – March 2026. 1, 3.1

Mint, "Ola Electric's service crisis: mounting complaints and slipping market share," https://www.livemint.com/companies/ola-electric-service-crisis-bajaj-auto-tvs-motor-battery-ev-market-share-complaints-customer-html 2024. 18 September 2024; cites internal documents to estimate about 80,000 monthly service complaints across Ola's installed base. 1, 2

Mobility Outlook, "E2-Wheelers' Growth Relies On Subsidies, Localisation," https://www.mobilityoutlook.com/features/e2-wheelers-growth-relies-on-subsidies-localisation/ 2024. 2

Muehlegger, Erich and David S. Rapson, "Subsidizing Low- and Middle-Income Adoption of Electric Vehicles: Quasi-Experimental Evidence from California," *Journal of Public Economics*, 2022, *216*, 104752. 1

NITI Aayog and Rocky Mountain Institute, "India's Electric Mobility Transformation: Progress to Date and Future Opportunities," Technical Report, NITI Aayog, Government of India, New Delhi 2019. 1

Ola Electric, "Service-network site listings, Ola Electric maps API," Captured by the Internet Archive Wayback Machine, 3 January 2024. https://web.archive.org/web/2024/https://olaelectric.com 2024. Site-level listings of dedicated service centres, experience centres, and charging locations; 432 dedicated service centres with 98% coordinate-verified locations. 4

Rapson, David S. and Erich Muehlegger, "The Economics of Electric Vehicles," *Review of Environmental Economics and Policy*, 2023, *17* (2), 274–294. 1, 1

Reuters, "India orders audit of Ola's service centres after consumer complaints, source and document reveal," By Aditi Shah, 10 October 2024. https://sg.finance.yahoo.com/news/india-orders-audit-olas-centres-072402332.html 2024. Reports a September 2024 HSBC note whose analysts visited multiple Ola service hubs and found most "overwhelmed by the service requests", attributing the strain to under-investment in servicing capacity relative to volumes sold. 1, 2

Rezvani, Zeinab, Johan Jansson, and Jan Bodin, "Advances in Consumer Electric Vehicle Adoption Research: A Review and Research Agenda," *Transportation Research Part D: Transport and Environment*, 2015, *34*, 122–136. 1

Rhee, Mooweon and Pamela R. Haunschild, "The Liability of Good Reputation: A Study of Product Recalls in the U.S. Automobile Industry," *Organization Science*, 2006, *17* (1), 101–117. 1

Shapiro, Carl, "Premiums for High Quality Products as Returns to Reputations," *The Quarterly Journal of Economics*, 1983, *98* (4), 659–679. 1

Springel, Katalin, "Network Externality and Subsidy Structure in Two-Sided Markets: Evidence from Electric Vehicle Incentives," *American Economic Journal: Economic Policy*, 2021, *13* (4), 393–432. 1, 1

Tirole, Jean, "A theory of collective reputations (with applications to the persistence of corruption and to firm quality)," *Review of Economic Studies*, 1996, *63* (1), 1–22. 1

Xing, Jianwei, Benjamin Leard, and Shanjun Li, "What Does an Electric Vehicle Replace?," *Journal of Environmental Economics and Management*, 2021, *107*, 102432. 1

Part I

Appendix

Table of Contents

A Robustness Checks **32**

A.1 Alternative exposure: $\sinh^{-1}$(cumulative count) 32

A.2 Alternative outcome: $\sinh^{-1}$(registrations) 33

A.3 Synthetic difference-in-differences diagnostics and placebo distribution 34

A.4 Pre-shock balance by exposure quartile 36

A.5 Region × segment × time fixed effects 37

A.6 State × segment × time fixed effects 39

A.7 Dose-response across exposure quintiles 41

A.8 Short-run and longer-run estimates 42

A.9 Donut window: dropping the two pre-treatment months 43

A.10 Zero-valued outcomes and log-like transformations 44

A.11 Placebo: the largest non-Ola brand 45

A.12 Adjacent electric-segment comparison: four-wheeler EVs 47

A.13 The registration shortfall and substitution toward ICE 48

A Robustness Checks

This appendix reports thirteen supplementary analyses. Sections A.1 and A.2 re-estimate the empirical designs using an alternative exposure measure or an alternative outcome transformation. In each case, the regression and SDID structures—including fixed effects, sample, clustering, weighting procedure, and quartile-partition rule—remain as in Section 3; only the exposure or outcome measure changes. The alternative exposure is constructed over April 2022–November 2023. All triple-difference robustness regressions retain the RTO $\times$ segment, RTO $\times$ month, and segment $\times$ month fixed effects used in the main specification. Section A.3 reports SDID weight and placebo diagnostics. Section A.4 examines pre-shock balance by exposure quartile. Sections A.5 and A.6 add region- and state-specific segment-month fixed effects. Section A.7 replaces the continuous exposure measure with quintile indicators. Section A.8 separates short- and longer-run post-periods. Section A.9 excludes the two transition months immediately before treatment. Section A.10 examines zero outcomes and log-like transformations. Section A.11 uses the pre-shock footprint of the largest non-Ola brand as a placebo exposure. Section A.12 compares non-Ola electric two-wheelers with four-wheeler EVs, and Section A.13 decomposes post-shock registration flows in high-exposure markets.

A.1 Alternative exposure: $\sinh^{-1}$(cumulative count)

The alternative triple-difference exposure is $\sinh^{-1}(\text{cumulative Ola count}_r)$ over April 2022–November 2023. This log-like transformation is defined at zero without the $+1$ adjustment used in $\log(1+x)$.

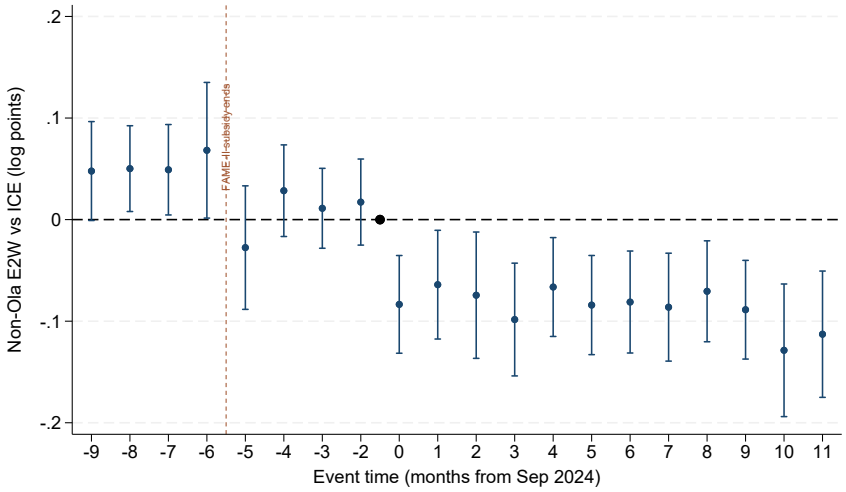
We do not report a separate SDID estimate for this transformation. SDID assigns treatment according to the top quartile of exposure, and $\sinh^{-1}(\cdot)$ is monotonic over non-negative values. The treated-control partition is therefore identical to that based on $\log(1+\text{cum Ola})$, and the SDID estimates are numerically unchanged from Table 2. We report this robustness check only for the triple-difference, where exposure enters linearly and the transformation changes the estimated slope.

Table A-1: Triple-difference estimates using $\sinh^{-1}$(Ola count) exposure

	Standard window		Donut window	
	No controls	Size/growth controls	No controls	Size/growth controls
Ola exp. $\times$ Post $\times$ Non-Ola	-0.063***	-0.114***	-0.068***	-0.132***
	(0.013)	(0.020)	(0.014)	(0.023)
Observations	37,212	37,212	33,668	33,668
Adj. R-sq	0.975	0.975	0.974	0.974

The sample, fixed effects, controls, and clustering are the same as in Table 1. Exposure is $\sinh^{-1}(\text{cum Ola}_r)$ measured over April 2022–November 2023. $^{*}\,p<0.10$, $^{**}\,p<0.05$, $^{***}\,p<0.01$.

Figure A-1: Event study using $\sinh^{-1}$(count) exposure



Notes: Event-study coefficients $\hat{\beta}_\tau$ from Equation (3.2), with exposure defined as $\sinh^{-1}(\text{cumulative Ola count}_r)$ over April 2022–November 2023 and with segment-specific $B_r \times \textit{Post}$ controls. The sample window is December 2023–August 2025, and August 2024 ($\tau = -1$) is the reference month. The vertical dashed line marks the expiry of the FAME-II purchase subsidy (31 March 2024). Error bars are 95% confidence intervals based on standard errors clustered by RTO and state × month.

A.2 Alternative outcome: $\sinh^{-1}$(registrations)

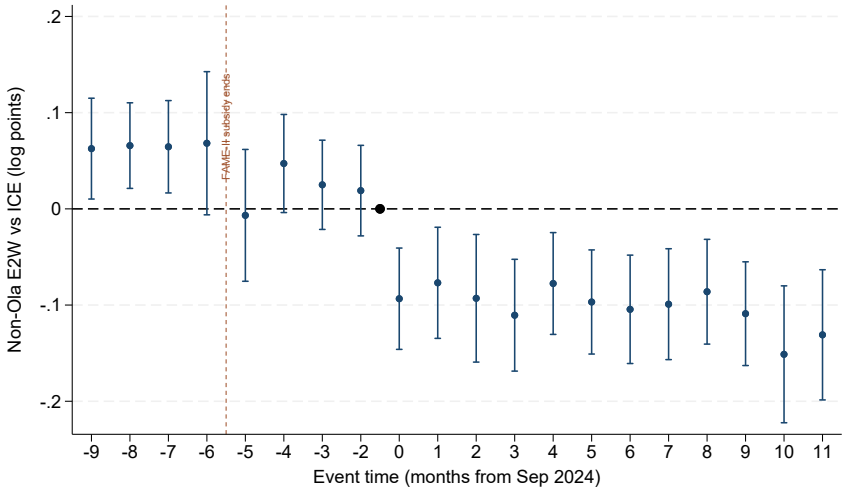
We replace $\log(\text{registrations} + 1)$ with $\sinh^{-1}(\text{registrations})$ while retaining the baseline exposure measure. This exercise assesses whether the estimates are sensitive to the choice between two common log-like transformations. We apply the alternative outcome to both empirical designs.

Table A-2: Triple-difference estimates using a $\sinh^{-1}$ outcome

	Standard window		Donut window	
	No controls	Size/growth controls	No controls	Size/growth controls
Ola exp. × Post × Non-Ola	-0.087***	-0.141***	-0.095***	-0.162***
	(0.014)	(0.022)	(0.016)	(0.025)
Observations	37,212	37,212	33,668	33,668
Adj. R-sq	0.971	0.971	0.970	0.971

The sample, fixed effects, controls, clustering, and baseline exposure are the same as in Table 1. The outcome is $\sinh^{-1}(\text{registrations})$ rather than $\log(\text{registrations} + 1)$. The reported coefficient is the non-Ola-electric-versus-ICE triple-difference. $^{*}\,p < 0.10$, $^{**}\,p < 0.05$, $^{***}\,p < 0.01$.

Figure A-2: Event study using a $\sinh^{-1}$ outcome



Notes: Event-study coefficients $\hat{\beta}_\tau$ from Equation (3.2), retaining the baseline *Ola Exposure*$_r$ and the segment-specific $B_r \times Post$ controls but replacing $\log(\text{registrations}+1)$ with $\sinh^{-1}(\text{registrations})$. The sample window is December 2023–August 2025, and August 2024 ($\tau = -1$) is the reference month. The vertical dashed line marks the expiry of the FAME-II purchase subsidy (31 March 2024). Error bars are 95% confidence intervals based on standard errors clustered by RTO and state × month.

Table A-3: Synthetic difference-in-differences using a $\sinh^{-1}$ outcome

	(1) Non-Ola electric 2W	(2) All electric 2W
ATT	-0.224***	-0.135***
	(0.034)	(0.024)
95% CI	[-0.290, -0.157]	[-0.183, -0.087]
Treated areas	221	221
Control areas	665	665
Months	21	21
Placebo reps	1,000	1,000

The sample window, exposure partition, and inference procedure are the same as in Table 2. Outcomes are $\sinh^{-1}(\text{registrations})$ rather than $\log(\text{registrations}+1)$. $^{*}\,p<0.10$, $^{**}\,p<0.05$, $^{***}\,p<0.01$.

A.3 Synthetic difference-in-differences diagnostics and placebo distribution

For the main SDID estimates in Table 2, we report two additional diagnostics. Table A-4 summarizes the distribution of synthetic-control weights and the pre-period prediction error: the effective number of control RTOs, calculated as $1/\sum_i \hat{\omega}_i^2$; the maximum weight assigned to any control RTO; and the pre-period root-mean-squared prediction error. For both outcomes, the weights are diffuse across the 665 controls, with several hundred effective control units and no individual

weight above 0.7%. Thus, the estimates are not driven by a small number of heavily weighted RTOs.

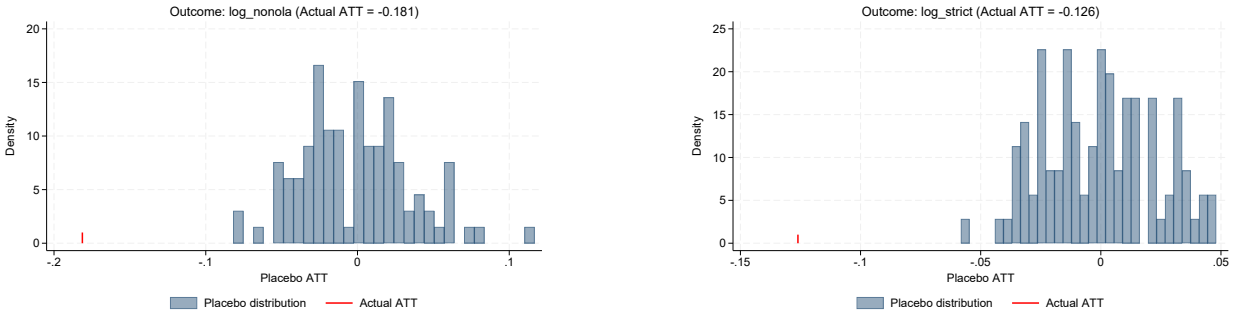
Figure A-3 displays placebo ATT distributions obtained by randomly assigning the treated label to subsets of the 665 control RTOs and re-estimating SDID. Each panel contains 100 placebo assignments, and the vertical red line marks the actual ATT. For both outcomes, the actual estimate lies well below the placebo distribution, consistent with the small placebo standard errors and the 1% significance levels reported in Table 2.

Table A-4: SDID diagnostics: weight concentration and placebo inference

	(1) Non-Ola electric 2W	(2) All electric 2W
Effective N control units	646.2	598.0
Max single-unit weight	0.003	0.004
Pre-period RMSPE	1.9044	1.7865
Number of treated areas (Q4)	221	221
Number of control areas (Q1-Q3)	665	665
Placebo replications	100	100

Diagnostics correspond to the SDID estimates in Table 2. "Effective N control units" is $1/\sum_i \hat{\omega}_i^2$ for the optimal control weights, which sum to one over the 665 controls. "Max single-unit weight" is $\max_i \hat{\omega}_i$. "Pre-period RMSPE" is the root-mean-squared treated-minus-synthetic difference over December 2023–August 2024. Because SDID includes unit fixed effects, raw treated and synthetic levels need not coincide; the RMSPE should be interpreted in that context. The placebo-replication row refers to the 100 manual reassignments plotted in Figure A-3, not the $1{,}000$ reassignments used for inference in Table 2.

Figure A-3: SDID placebo ATT distributions



(a) $\log(\text{Non-Ola electric} + 1)$ (b) $\log(\text{All electric} + 1)$

Notes: Each panel reports 100 placebo ATTs generated by assigning the 221-RTO treated label to a random subset of the 665 controls and re-estimating SDID. The histogram shows the placebo distribution, and the red line marks the actual ATT from Table 2. These manual placebo assignments are separate from the $1{,}000$ reassignments used for inference in Table 2.

A.4 Pre-shock balance by exposure quartile

Table A-5 reports pre-shock means for ten RTO characteristics by quartile of $\log(1 + \textit{cum Ola})$ measured over April 2022–November 2023. It also reports Imbens–Rubin normalised differences comparing the top quartile (Q_4) with Q_1 and with Q_1–Q_3 pooled. Following Imbens and Rubin (2015), absolute normalised differences above 0.25 indicate substantively important imbalance, whereas smaller values indicate that the standardised mean difference is modest relative to within-group dispersion.

High-exposure RTOs are systematically larger and more mature EV markets. Relative to Q_1, Q_4 has larger two-wheeler markets (ND $= 1.44$), higher pre-shock EV shares (ND $= 1.22$), a larger Ola share within EVs (ND $= 1.53$), and more non-Ola electric brands (ND $= 2.51$). These differences are expected because Ola initially expanded more heavily in large urban markets; cumulative Ola registrations are therefore mechanically related to market size and EV maturity.

Two features partially mitigate, but do not eliminate, concerns arising from these imbalances. First, several pre-shock outcome trends most directly related to the spillover are balanced or nearly balanced: the total two-wheeler growth ratio (ND $= -0.11$ and -0.06), total two-wheeler year-on-year growth (ND $= -0.15$ and -0.11), and ICE year-on-year growth (ND $= -0.27$ and -0.14). Non-Ola E2W year-on-year growth is more imbalanced (ND $= 0.67$ and 0.44), motivating the pre-determined size and growth controls interacted with post and segment. Second, the fixed-effect structure absorbs persistent RTO-by-segment level differences and all RTO-month shocks common to the two segments. The $B_r \times \textit{Post}$ controls additionally allow pre-shock size and growth to have different post-period associations with the two segments. Appendix A.5 further absorbs region $\times$ segment $\times$ month variation to address the spatial concentration shown in Figure 3. These adjustments do not make exposure as-good-as-random, but they reduce several observable sources of differential trends.

Table A-5: Pre-shock balance by Ola-exposure quartile

	Ola-exposure quartile				Normalized difference	
	Q_1	Q_2	Q_3	Q_4	Q_4 vs. Q_1	Q_4 vs. lower 75%
log(pre-shock monthly 2W size)	9.45	9.79	9.99	10.58	1.442	1.089
Pre-shock total 2W growth ratio	1.08	1.12	1.07	1.07	-0.112	-0.062
Pre-shock total 2W YoY growth (log-pp)	0.08	0.10	0.06	0.04	-0.149	-0.113
EV share of 2W, %	2.41	2.95	4.53	9.11	1.216	1.032
Ola share of EV, %	14.29	25.17	27.88	31.62	1.527	0.696
Ola share of 2W, %	0.27	0.62	1.15	3.15	0.601	0.513
Non-Ola E2W YoY growth (log-pp)	-0.44	-0.21	-0.13	0.06	0.671	0.438
Ola YoY growth (log-pp)	0.59	0.86	0.68	0.51	-0.089	-0.228
ICE YoY growth (log-pp)	0.09	0.10	0.05	0.04	-0.273	-0.136
Distinct non-Ola E2W brands	9.48	11.71	15.09	22.17	2.506	1.823
Mean log(1+cum Ola)	3.22	4.42	5.31	6.77	—	—
Number of areas	225	218	222	221	—	—
Number of states represented	24	23	22	21	—	—

Notes: The sample contains 886 size-filtered RTOs with non-zero pre-shock Ola exposure. Quartiles are based on $\log(1 + \textit{cum Ola}_r)$ measured over April 2022–November 2023, with Q_1 the lowest and Q_4 the highest. The last two columns report the Imbens–Rubin normalised difference $(\bar{X}_T - \bar{X}_C)/\sqrt{(s_T^2 + s_C^2)/2}$, comparing Q_4 with Q_1 and with the pooled lower three quartiles, respectively. Absolute values above 0.25 indicate substantive imbalance. Growth-ratio and year-on-year rows measure pre-shock registration changes by segment, using late versus early pre-periods and September–November 2023 versus September–November 2022. "Distinct non-Ola E2W brands" counts brands with at least one pre-shock registration in the RTO.

A.5 Region × segment × time fixed effects

A concern in continuous-exposure triple-difference designs is that geographically concentrated exposure may proxy for region-specific shocks. High-Ola RTOs are disproportionately located in southern and western India, regions that differ from the north and east in baseline EV penetration, charging infrastructure, uptake of FAME-II and EMPS, and ICE replacement cycles. If non-Ola electric registrations were already following different paths relative to ICE in those regions for reasons unrelated to Ola, the baseline estimate could combine those regional dynamics with the post-crisis exposure gradient.

We therefore add a fourth fixed-effect dimension, τ_{Rft}, comprising a separate intercept for every region × segment × month cell, where region is one of four Indian zones (north, south, east, or west).[1] These fixed effects allow the non-Ola-electric-versus-ICE gap to follow an unrestricted monthly path within each region, absorbing region-month shocks with different effects across the two segments. The coefficient is then identified from within-region variation in cumulative pre-shock Ola exposure interacted with post and segment.

Table A-6 compares the baseline and region-adjusted estimates in the standard and donut windows. In the standard window with $B_r \times \textit{Post}$ controls, the coefficient declines in magnitude from

[1]North: CH, DL, HR, HP, JK, LA, PB, RJ, UK, UP. South: AN, AP, KA, KL, LD, PY, TG, TN. East: AR, AS, BR, JH, ML, MN, MZ, NL, OR, SK, TR, WB. West: CG, DD, GA, GJ, MH, MP. The sample contains 212 northern, 390 southern, 119 eastern, and 165 western RTOs.

-0.118 to -0.091 after adding region $\times$ segment $\times$ month fixed effects—a reduction of about one-fifth—and remains statistically significant ($p < 0.01$). The donut estimates show a similar change, from -0.136 to -0.108. Thus, the within-region estimate is approximately four-fifths of the baseline magnitude. Figure A-4 presents the corresponding event study with $B_r \times \textit{Post}$ controls. The eight pre-period coefficients are jointly indistinguishable from zero ($F(8, 566) = 1.54$, $p = 0.14$), while all post-period coefficients are negative and ten of twelve are individually significant. The region effects therefore absorb part of the geographic variation without eliminating the post-shock differential.

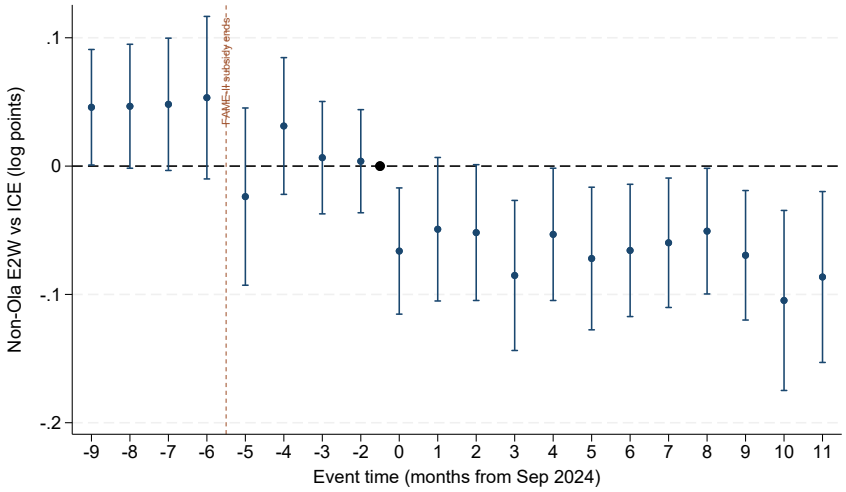
Region fixed effects provide an intermediate geographic check. The exposure map in Figure 3 shows concentration in the southern and western zones, and the four-zone interactions directly absorb segment-specific monthly paths at that spatial scale while preserving substantial within-zone exposure variation. The more restrictive state $\times$ segment $\times$ month specification in Appendix A.6 uses only within-state variation. In that specification, a single continuous slope is smaller, while top-quartile and top-quintile contrasts remain negative and statistically significant (Table A-8). The region specification should therefore be interpreted as a useful, but not definitive, balance between geographic flexibility and support for estimating a continuous gradient.

Table A-6: Triple-difference estimates with region-by-segment-by-month fixed effects

	Standard window				Donut window			
	No controls	Size/growth controls	Regional segment-time effects	Both	No controls	Size/growth controls	Regional segment-time effects	Both
Ola exp. × Post × Non-Ola	-0.065***	-0.118***	-0.053***	-0.091***	-0.071***	-0.136***	-0.059***	-0.108***
	(0.013)	(0.021)	(0.014)	(0.022)	(0.015)	(0.023)	(0.016)	(0.025)
Observations	37,212	37,212	37,212	37,212	33,668	33,668	33,668	33,668
Adj. R-sq	0.975	0.975	0.976	0.976	0.974	0.974	0.975	0.975

Notes: The baseline sample, controls, and clustering follow Table 1. Columns (1)–(4) use the standard window (December 2023–August 2025), and columns (5)–(8) use the donut window, which excludes July and August 2024. Within each window, the first two columns report the baseline without and with $B_r \times \textit{Post}$ controls; the third adds region $\times$ segment $\times$ month fixed effects; and the fourth includes both the region effects and controls. Region is one of four zones: North, South, East, or West. $^{*}\, p < 0.10$, $^{**}\, p < 0.05$, $^{***}\, p < 0.01$.

Figure A-4: Event study with region-by-segment-by-month fixed effects



Notes: Event-study estimates $\hat{\beta}_\tau$ from Equation (3.2), adding region $\times$ segment $\times$ month fixed effects for four Indian zones and retaining the segment-specific $B_r \times \textit{Post}$ controls. The sample window is December 2023–August 2025, and August 2024 ($\tau = -1$) is the reference month. The vertical dashed line marks the expiry of the FAME-II purchase subsidy (31 March 2024). A joint test does not reject that the eight pre-period coefficients equal zero ($F(8, 566) = 1.54$, $p = 0.14$). Error bars are 95% confidence intervals based on standard errors clustered by RTO and state $\times$ month.

A.6 State $\times$ segment $\times$ time fixed effects

The region specification absorbs trends common to broad zones, but several EV policies are administered at the state level. Road-tax waivers, registration-fee exemptions, and supplementary purchase subsidies differ across states and may change on state-specific schedules. We therefore replace the four-zone effects with state $\times$ segment $\times$ month fixed effects. The exposure coefficient is then identified only by comparing RTOs within the same state, segment, and month. States represented by a single RTO provide no within-state variation and are omitted; this removes two states and 84 observations from the standard-window sample.

Table A-7 reports the linear specification. Relative to the region-adjusted estimates, the continuous-exposure coefficient is smaller: without predetermined controls, it is -0.042 in the standard window and -0.045 in the donut window, both significant at 1%; with $B_r \times \textit{Post}$ controls, it is -0.047 and -0.051, respectively, both significant at 10%. These estimates show that the linear gradient is attenuated within states. They do not, however, imply that all high-exposure contrasts disappear. As Appendix A.7 shows, the response is concentrated at the top of the exposure distribution. Within-state exposure support is dominated by lower-exposure RTOs, where the estimated response is comparatively flat, so a constant linear slope can be substantially smaller than upper-tail contrasts.

To examine functional form, Table A-8 estimates three versions of the triple-difference—a continuous exposure term, a top-quartile indicator, and a top-quintile indicator—with and without state $\times$ segment $\times$ month fixed effects. Two patterns emerge. First, the response is nonlinear:

Table A-7: Triple-difference estimates with state-by-segment-by-month fixed effects

	Standard window				Donut window			
	No controls	Size/growth controls	State segment-time effects	Both	No controls	Size/growth controls	State segment-time effects	Both
Ola exp x Post x Non-Ola	-0.065***	-0.118***	-0.042***	-0.047*	-0.071***	-0.136***	-0.045***	-0.051*
	(0.013)	(0.021)	(0.013)	(0.025)	(0.015)	(0.023)	(0.016)	(0.029)
Observations	37,212	37,212	37,128	37,128	33,668	33,668	33,592	33,592
Adj R-sq	0.975	0.975	0.979	0.979	0.974	0.974	0.978	0.978

Notes: The baseline specification, controls, and clustering follow Table 1. "State segment-time effects" adds state × segment × month fixed effects, so identification comes only from RTOs within the same state and monthly policy environment; "Both" also includes the predetermined size and growth controls. Two single-RTO states are omitted. The standard window is December 2023–August 2025. The donut window additionally excludes July and August 2024. $^{*}\,p < 0.10$, $^{**}\,p < 0.05$, $^{***}\,p < 0.01$.

Figure A-5 shows little difference in the lower three quintiles and larger negative estimates in the top two quintiles. The pooled top-quartile and top-quintile coefficients are -0.394 and -0.437, respectively, larger than a constant per-log-unit slope would imply for the corresponding contrasts. Second, the upper-tail coefficients remain negative and statistically significant within states. Relative to lower-exposure RTOs in the same state, the estimated non-Ola registration shortfall is -0.196 for the top quartile and -0.209 for the top quintile, both significant at 1% ($t \simeq -4.9$) and approximately half the pooled magnitudes. These comparisons use the twenty states containing both top-quartile and lower-exposure RTOs, so no single state identifies the result. The evidence therefore indicates that the small within-state linear coefficient partly reflects the mismatch between a constant slope and a threshold-like response.

Table A-8: Functional form and within-state triple-difference estimates

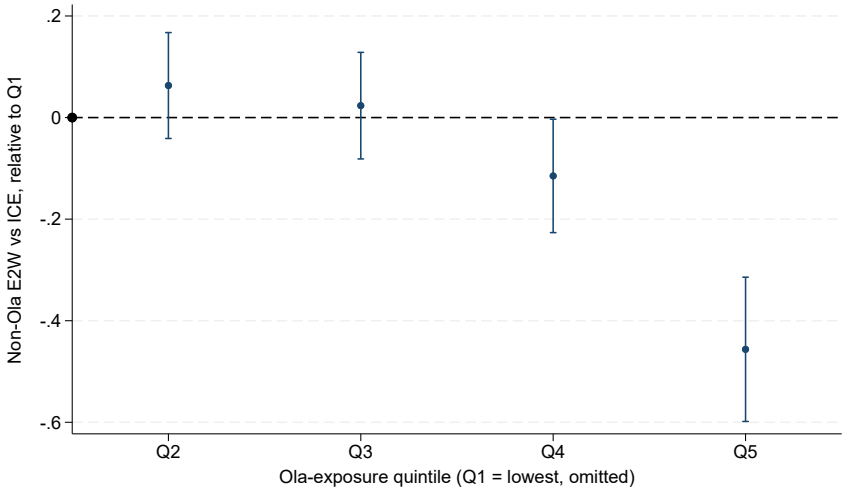
	Pooled comparison Standard fixed effects	Within-state comparison State-specific segment-time effects
Ola exposure (linear, per log unit)	-0.118^{***}	-0.047^{*}
	(0.021)	(0.025)
Top-quartile indicator (vs. rest)	-0.394^{***}	-0.196^{***}
	(0.047)	(0.040)
Top-quintile indicator (vs. rest)	-0.437^{***}	-0.209^{***}
	(0.051)	(0.043)
Observations	37,212	37,128

Notes: All specifications use the standard December 2023–August 2025 window and include $B_r \times Post$ controls. Each cell is a separate triple-difference with outcome $\log(registrations + 1)$; the reported coefficient interacts the row-specific exposure measure with $Post_t$ and the non-Ola-electric indicator. Row 1 uses continuous $Ola\ Exposure_r$ per log unit; rows 2 and 3 use top-quartile and top-quintile indicators. "Pooled" includes the baseline three-way fixed effects. "Within-state" additionally includes state × segment × month fixed effects and is identified by the twenty states containing both high- and lower-exposure RTOs. Standard errors are two-way clustered by RTO and state × month. $^{*}\,p < 0.10$, $^{**}\,p < 0.05$, $^{***}\,p < 0.01$.

A.7 Dose-response across exposure quintiles

The baseline specification imposes a single linear exposure slope. To assess this restriction, we replace the continuous interaction with indicators for the RTO's exposure quintile, each interacted with $Post_t$ and the non-Ola-electric indicator; the least-exposed quintile, Q_1, is omitted. Figure A-5 and Table A-9 show little estimated difference between Q_2 or Q_3 and Q_1, a negative coefficient in Q_4, and the largest negative coefficient in Q_5. The estimated response is therefore concentrated among RTOs with high pre-shock Ola exposure rather than distributed uniformly across the exposure range.

Figure A-5: Dose-response of non-Ola electric registrations relative to ICE



Notes: Coefficients on exposure-quintile $\times$ $Post_t$ $\times$ non-Ola-electric indicators from the standard-window version of Equation (3.2), with Q_1 omitted and $B_r \times Post$ controls included. Mean log exposure by quintile is 3.1, 4.2, 4.9, 5.6, and 7.0 for Q_1 through Q_5, respectively. Error bars are 95% confidence intervals based on standard errors clustered by RTO and state $\times$ month.

Table A-9: Dose-response coefficients by exposure quintile

	Standard window	Donut window
Q2 x Post x Non-Ola	0.063	0.063
	(0.053)	(0.059)
Q3 x Post x Non-Ola	0.023	0.022
	(0.053)	(0.060)
Q4 x Post x Non-Ola	-0.115**	-0.144**
	(0.057)	(0.063)
Q5 x Post x Non-Ola	-0.456***	-0.533***
	(0.072)	(0.078)
Observations	37,212	33,668
Adj R-sq	0.975	0.975

Notes: The triple-difference replaces continuous exposure with quintile indicators and omits Q_1. Fixed effects, $B_r \times Post$ controls, and clustering are the same as in Table 1. $^{*}\, p < 0.10$, $^{**}\, p < 0.05$, $^{***}\, p < 0.01$.

A.8 Short-run and longer-run estimates

The main estimates average over the first twelve months after the shock. Registration data through March 2026 add seven months. We divide the post-period into a short-run interval (September 2024–August 2025) and a longer-run interval (September 2025–March 2026), allow the exposure interaction to differ across the two intervals, and test whether the coefficients are equal. The reported outcome is the non-Ola electric segment relative to ICE.

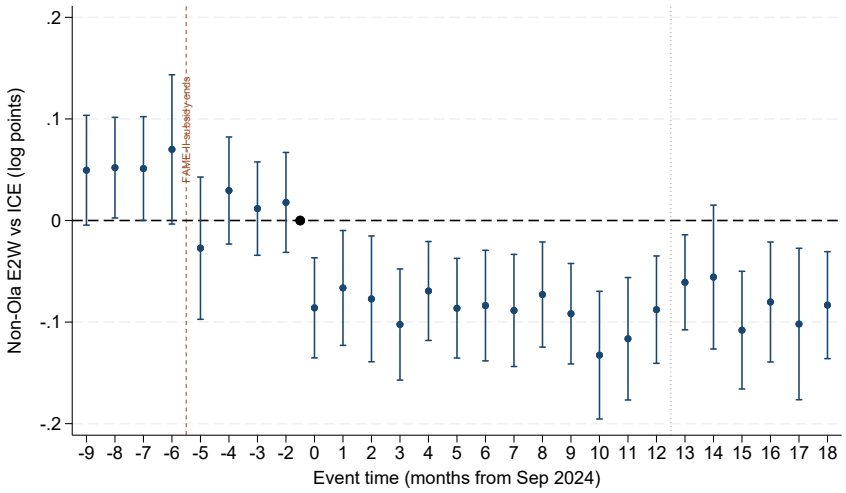
Table A-10 and Figure A-6 show similar estimates across the two intervals: -0.118 in the first post-year and -0.111 in the subsequent seven months. The equality test does not reject ($p = 0.53$). Thus, the negative exposure gradient does not visibly attenuate or deepen through March 2026. This longer-horizon pattern should be interpreted cautiously. The later period includes additional potential confounders, such as new non-Ola models and state-policy changes in 2025, that the design may not fully separate from the original shock. The split therefore describes persistence in the observed trajectory rather than providing an equally clean causal estimate at the longer horizon.

Table A-10: Short-run and longer-run triple-difference estimates

	Exposure gradient: non-Ola electric 2W relative to ICE 2W
September 2024–August 2025	-0.118***
	(0.020)
September 2025–March 2026	-0.111***
	(0.022)
p-value: equal coefficients	0.526
Observations	49,612
Adj R-sq	0.976

Notes: Equation (3.2) is estimated on a panel extended through March 2026, replacing the single post interaction with short-run (September 2024–August 2025) and longer-run (September 2025–March 2026) interactions. The specification includes the baseline three-way fixed effects and predetermined size and growth controls. "p-value: equal coefficients" reports the Wald test of equality between the two period-specific coefficients. * $p < 0.10$, ** $p < 0.05$, *** $p < 0.01$.

Figure A-6: Extended event study through March 2026



Notes: Event-time coefficients $\hat{\beta}_\tau$ from Equation (3.2), estimated through March 2026 (event time $+18$) with the baseline three-way fixed effects and segment-specific $B_r \times Post$ controls. August 2024 ($\tau = -1$) is the reference month. The dotted vertical line at $\tau = 12$ marks September 2025, the beginning of the longer-run interval. The dashed vertical line in the pre-period marks the expiry of the FAME-II purchase subsidy (31 March 2024). Error bars are 95% confidence intervals based on standard errors clustered by RTO and state $\times$ month.

A.9 Donut window: dropping the two pre-treatment months

Ola registrations were already declining in July and August 2024, the two months immediately before the September treatment date (Figure 2). If consumers in high-exposure markets began responding during these transition months, including them could blur the pre/post contrast. The donut specification excludes July and August 2024, so the pre-period ends in June and the post-period begins in September. Table A-11 re-estimates the static models in Table 1, and Figure A-7 reports the corresponding event study.

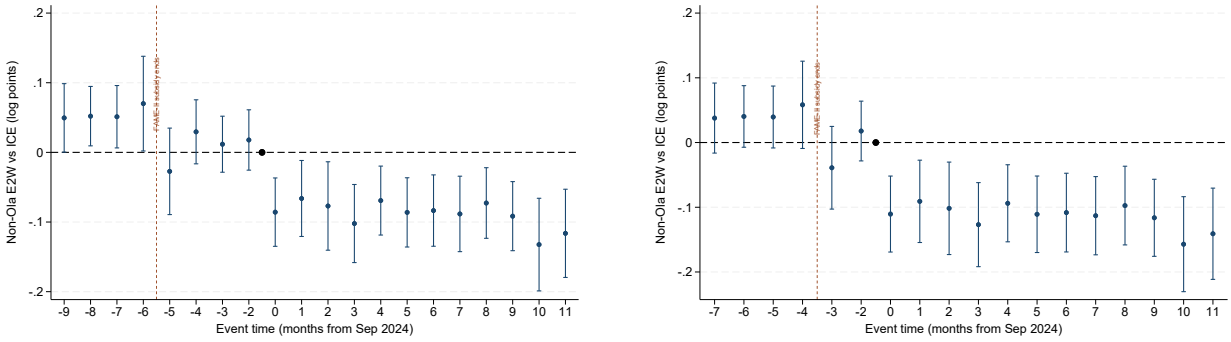
The controlled coefficient is slightly larger in magnitude in the donut window: -0.136 compared with -0.118 in the standard window. The uncontrolled and month-varying-control estimates change in the same direction. Excluding the two transition months therefore does not account for the negative post-shock exposure gradient.

Table A-11: Static triple-difference estimates excluding July and August 2024

	No controls	Size/growth controls	Month-specific controls
Ola exp. × Post × Non-Ola	-0.071***	-0.136***	-0.136***
	(0.015)	(0.023)	(0.023)
Observations	33,668	33,668	33,668
Adjusted R-squared	0.974	0.974	0.975

Notes: Table 1 is re-estimated after excluding July and August 2024. The sample, fixed effects, controls, and clustering are otherwise unchanged. "No controls" includes only the exposure interaction. "Size/growth controls" allows predetermined RTO size and growth to have segment-specific post-period associations. "Month-specific controls" allows these segment-specific associations to vary by calendar month. $^{*}\,p < 0.10$, $^{**}\,p < 0.05$, $^{***}\,p < 0.01$.

Figure A-7: Event-study estimates in the standard and donut windows



(a) Standard window

(b) Donut window (drops Jul–Aug 2024)

Notes: Event-study coefficients $\hat{\beta}_\tau$ from Equation (3.2), with the baseline three-way fixed effects and segment-specific $B_r \times \textit{Post}$ controls. Panel (a) reproduces the standard December 2023–August 2025 window from Figure 4 and uses August 2024 ($\tau = -1$) as the reference month. Panel (b) excludes July and August 2024 and therefore uses June 2024 ($\tau = -3$), the final retained pre-treatment month, as the reference month; its earliest lead is $\tau = -9$. In both panels the vertical dashed line marks the expiry of the FAME-II purchase subsidy (31 March 2024). Error bars are 95% confidence intervals based on standard errors clustered by RTO and state × month. The post-period paths are similar across the two windows.

A.10 Zero-valued outcomes and log-like transformations

The main specifications use $\log(Y+1)$, and a small fraction of registration cells have zero outcomes. Chen and Roth (2024) show that, when zeros are present, log-like transformations need not have a scale-invariant percentage interpretation because their implicit weighting of the extensive margin can depend on the units of measurement. This concern is most relevant when zeros are common or when treatment changes the probability that Y is positive. We examine both conditions directly.

Zero outcomes are uncommon. Table A-12 reports that 1.3% of monthly non-Ola electric cells are zero, no ICE cells are zero, and the pooled zero share is 0.6%. Aggregating to two-month bins reduces the corresponding shares to 0.4% and 0.2%. The sample restriction requiring at least 100 cumulative electric two-wheeler registrations removes many thin markets in which zeros would otherwise be concentrated.

The extensive margin is also stable in treated RTOs. Table A-13 shows that the non-Ola electric zero share in control RTOs declines from 2.9% before treatment to 0.6% afterward, while the treated share changes from 0.5% to 0.3%. Treated RTOs have positive non-Ola registrations in 99.5–99.7% of cells throughout the sample. The limited extensive-margin change occurs primarily in lower-exposure control markets as the category expands.

These patterns indicate that the estimated spillover is primarily an intensive-margin result: non-Ola registrations grow more slowly in high-exposure markets that already have positive registrations. Because $\log(Y+1)$ is applied almost entirely to positive cells, most with tens or hundreds of registrations, the scale sensitivity emphasized by Chen and Roth (2024) is unlikely to be the principal source of the estimates. Consistent with this interpretation, replacing $\log(Y+1)$ with $\sinh^{-1}(Y)$ in Appendix A.2 leaves the coefficient negative and statistically significant.

Table A-12: Share of outcome cells equal to zero

Cell definition	Non-Ola electric 2W	ICE 2W	Both segments
Monthly (RTO × segment × month)	1.3%	0.0%	0.6%
Bi-monthly (RTO × segment × bin)	0.4%	0.0%	0.2%

Notes: Share of outcome cells equal to zero in the 886-RTO estimation sample, reported by frequency and segment. "Both segments" combines the non-Ola electric and ICE observations. A two-month bin is classified as zero only when both constituent monthly observations are zero.

Table A-13: Non-Ola electric zero shares by exposure group and period

Exposure group	Pre-crisis	Post-crisis	Change (pp)
Lower exposure	2.9%	0.6%	−2.3
High exposure	0.5%	0.3%	−0.2

Notes: Monthly share of non-Ola electric two-wheeler cells equal to zero. Treated RTOs are in the top quartile of pre-shock Ola exposure; control RTOs are in the lower three quartiles. The pre-period is December 2023–August 2024, and the post-period is September 2024–August 2025. "Change" is the post-minus-pre difference in percentage points.

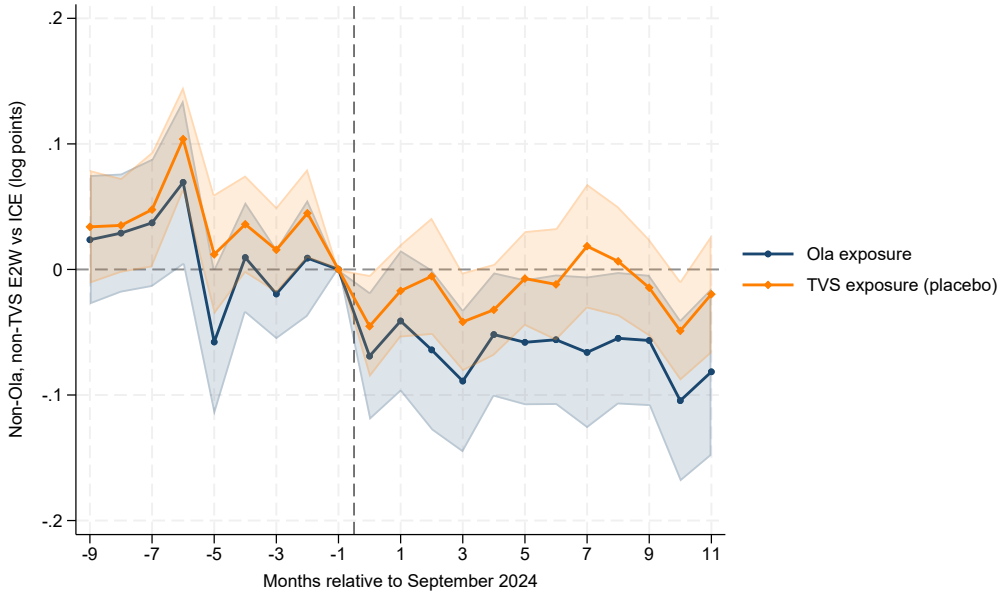
A.11 Placebo: the largest non-Ola brand

A remaining concern is that Ola exposure may proxy for the geography of large electric two-wheeler incumbents generally rather than for Ola's reputational shock specifically. Markets with a large Ola presence were also more developed EV markets, so the pre-shock footprints of other major brands are spatially correlated with Ola's. We examine this concern using a brand-level

placebo. We replace Ola exposure with $\log(1 + \text{cum TVS}_r)$, the predetermined installed base of TVS over April 2022–November 2023. TVS was the second-largest electric two-wheeler brand during this period and did not experience a comparable reputational event in the sample window. To avoid mechanically relating a brand's own registrations to its exposure, the outcome excludes both Ola and TVS and equals $\log(Y+1)$ for all remaining electric two-wheelers, differenced against ICE. The sample, fixed effects, $B_r \times \textit{Post}$ controls, and clustering are otherwise identical to the baseline triple-difference.

Figure A-8 overlays event-study coefficients for the Ola and TVS gradients using this common outcome. The gradients co-move before treatment, as expected given their overlapping geography, and both become negative after September 2024. Thus, the footprint of a non-shocked incumbent also predicts some post-period variation in these registrations. The two paths differ in persistence: the Ola gradient stabilises near -0.06 log points and remains negative through August 2025, whereas the TVS gradient is smaller and moves toward zero after several months. The corresponding static coefficients are -0.077 for Ola and -0.055 for TVS. Because the confidence intervals overlap throughout, this difference is suggestive rather than statistically decisive. It is nevertheless consistent with the more persistent component of the gradient being more closely associated with Ola's footprint than with incumbent geography generally.

Figure A-8: Brand-placebo event study: Ola and TVS exposure



Notes: Event-study triple-difference coefficients for pre-shock brand exposure interacted with calendar month and the electric-segment indicator, relative to August 2024. The navy series uses Ola exposure, $\log(1 + \text{cum Ola}_r)$, and the orange series uses TVS exposure, $\log(1 + \text{cum TVS}_r)$; both are measured over April 2022–November 2023. The outcome is the log count of electric two-wheelers excluding both Ola and TVS, differenced against ICE registrations. The sample, fixed effects, $B_r \times \textit{Post}$ controls, and clustering follow Table 1. Shaded areas are 95% confidence intervals based on standard errors clustered by RTO and state × month.

A.12 Adjacent electric-segment comparison: four-wheeler EVs

Four-wheeler electric vehicles provide a within-electric comparison segment for the triple-difference: Ola produced no four-wheelers, so the segment shares local determinants of electric-vehicle demand without direct exposure to the shock. Equation (3.2) is re-estimated with $f \in \{$non-Ola electric two-wheeler
All other elements are unchanged: the predetermined *Ola Exposure*$_r$ from Equation (3.1); RTO $\times$ segment, RTO $\times$ month, and segment $\times$ month fixed effects; $B_r \cdot Post_t \cdot \mathbf{1}[f]$ controls; the December 2023–August 2025 sample window; and two-way clustering by RTO and state $\times$ month. Four-wheeler EV registrations are constructed from the same administrative source using electric-fuel four-wheeler vehicle classes. Because four-wheeler EV volume is approximately one-tenth of electric two-wheeler volume, Table A-14 also reports a Poisson pseudo-maximum-likelihood count specification.

The static coefficients are -0.129 without controls, -0.184 with $B_r \cdot Post$ controls, and -0.074 in the PPML specification; all are statistically significant at the 1% level. Figure 5 in the main text reports the event study. The comparison has two limitations. Two- and four-wheeler EVs serve different buyers and uses, differ substantially in price, and were subject to different policies; four-wheeler EVs were excluded from both EMPS and PM E-DRIVE (Ministry of Heavy Industries, 2024a,c). The comparison therefore cannot absorb all shocks specific to electric two-wheelers. In addition, the pre-trend test is marginal without the predetermined controls ($p = 0.08$), and the strongest pre-period fit is obtained after conditioning on size and growth. The September 2024 subsidy transition is unlikely to mechanically explain the immediate divergence because the electric two-wheeler incentive remained Rs. 5,000 per kWh under EMPS and during the first year of PM E-DRIVE, with the scheduled reduction beginning only in April 2025 (Autocar Professional, 2024c). That later reduction could, however, contribute to the widening gap near the end of the sample.

Table A-14: Non-Ola electric two-wheelers versus four-wheeler EVs

	Log outcome		Registration count
	No controls	Size/growth controls	PPML
Ola exp. $\times$ Post $\times$ Non-Ola E2W	-0.129***	-0.184***	-0.074***
	(0.014)	(0.020)	(0.021)
Observations	37,212	37,212	36,816
Adjusted R-squared	0.928	0.928	

Exposure, sample, fixed effects, controls, and clustering follow Table 1, but the comparison segment is four-wheeler EVs rather than ICE two-wheelers. The first two columns report log-outcome triple-difference estimates without and with $B_r \cdot Post$ controls; the third reports a PPML count estimate. $^{*}\, p < 0.10$, $^{**}\, p < 0.05$, $^{***}\, p < 0.01$.

A.13 The registration shortfall and substitution toward ICE

The main estimates show that non-Ola electric registrations fell below their counterfactual path in markets with greater pre-crisis Ola exposure. How many registrations does this shortfall represent, and could an increase in ICE registrations account for it? We estimate the changes in vehicle counts for the 221 RTOs in the top quartile of pre-crisis Ola exposure, using the 665 lower-exposure RTOs as the comparison group.

Let Y_{rft} denote registrations in RTO r, segment f, and month t, where the two segments are non-Ola electric and ICE two-wheelers. We estimate the following model by Poisson pseudo-maximum likelihood (PPML), with μ_{rft} denoting the expected registration count:

$$\mu_{rft} = \exp\left[\alpha_{rf} + \delta_{ft} + \theta_f(\mathit{High}_r \times \mathit{Post}_t) + B_r'\gamma_f \mathit{Post}_t\right]. \tag{A.1}$$

Here, High_r equals one for the top exposure quartile, and Post_t equals one from September 2024 onward. RTO-by-segment fixed effects α_{rf} absorb permanent differences in registration levels, while segment-by-month fixed effects δ_{ft} absorb the national monthly path of each segment. The vector B_r contains the predetermined, standardised market-size and growth controls defined in Section 3.2; their post-period associations, γ_f, are allowed to differ by segment. The two coefficients θ_f measure the post-crisis change in high-exposure RTOs relative to lower-exposure RTOs for non-Ola electric and ICE registrations separately. For each segment, $\exp(\theta_f)-1$ is the estimated proportional change relative to its counterfactual.

Estimation covers May 2024–August 2025, with four pre-crisis months following the April subsidy transition and twelve post-crisis months. Figure A-9 shows a comparatively flat pre-period for non-Ola electric registrations over this shorter window. Standard errors are two-way clustered by RTO and state $\times$ month. The model omits the RTO-by-month fixed effects used in the main triple-difference so that it can estimate each segment's change without using the other segment as a benchmark. Identification requires that, conditional on the controls, high- and lower-exposure RTOs would otherwise have followed parallel segment trends. For the regional and state specifications, we replace δ_{ft} with region-by-segment-by-month or state-by-segment-by-month fixed effects. These specifications compare high- and lower-exposure markets within the same region or state.

To obtain counterfactual registrations, we remove the estimated high-exposure interaction from Equation (A.1). For high-exposure RTOs during the post-crisis year, the national specification gives

$$\widehat{\mu}^0_{rft} = \exp\left[\widehat{\alpha}_{rf} + \widehat{\delta}_{ft} + B_r'\widehat{\gamma}_f\right]. \tag{A.2}$$

We sum these predictions across the 221 high-exposure RTOs and the twelve post-crisis months. Subtracting observed non-Ola electric registrations gives the estimated electric shortfall; subtracting predicted ICE registrations from observed ICE registrations gives the estimated ICE excess. The regional and state counterfactuals use their corresponding fixed effects. Because these predictions retain each segment's common monthly path, they measure the additional registration gap

associated with high exposure, rather than the nationwide effect of the crisis.

Panel A of Table A-15 reports 643,617 observed non-Ola electric registrations against 756,454 under the national counterfactual. The shortfall of 112,837 registrations is approximately 15% of expected registrations, with a 95% confidence interval of [46,500, 181,364]. Panel B shows that accounting for geography roughly halves the estimated shortfall: it falls to 52,077 under regional trends and 59,099 under state trends. The state estimate remains statistically distinguishable from zero, with a 95% interval of [20,290, 98,917]; the regional interval includes zero, [−2,104, 107,929]. A top-quintile exposure definition yields a shortfall of approximately 106,000 under the national counterfactual.

The ICE estimates do not establish whether these missing electric purchases shifted to petrol vehicles. Under the national counterfactual, ICE registrations are 36,311 below their predicted level; under regional and state trends, they are 123,088 and 134,185 above it. All three confidence intervals include zero and increases large enough to offset the corresponding non-Ola electric shortfall. This imprecision matters because the ICE market is much larger: the national counterfactual predicts 7.21 million ICE registrations, so an increase of only about 1.6% would absorb the entire 112,837 electric-registration shortfall. A statistically insignificant ICE response therefore cannot rule out substantial substitution.

Panel B also reports the residual obtained by subtracting excess ICE registrations from the non-Ola electric shortfall. Under national trends, both segments fall below their counterfactuals, giving a combined shortfall of 149,148. Under regional and state trends, the estimated ICE increase exceeds the non-Ola shortfall, making the residual negative. These residuals measure net registration gaps for the two reported segments; they do not count delayed or forgone purchases. An increase in ICE registrations cannot be attributed entirely to buyers switching from non-Ola electric vehicles, since other changes in local demand could also contribute. The exercise therefore quantifies the non-Ola registration shortfall, but cannot allocate it between substitution to ICE and postponed or forgone purchases.

Table A-15: Non-Ola electric-registration shortfalls and ICE registration changes

Panel A. Registrations in high-exposure RTOs, September 2024–August 2025

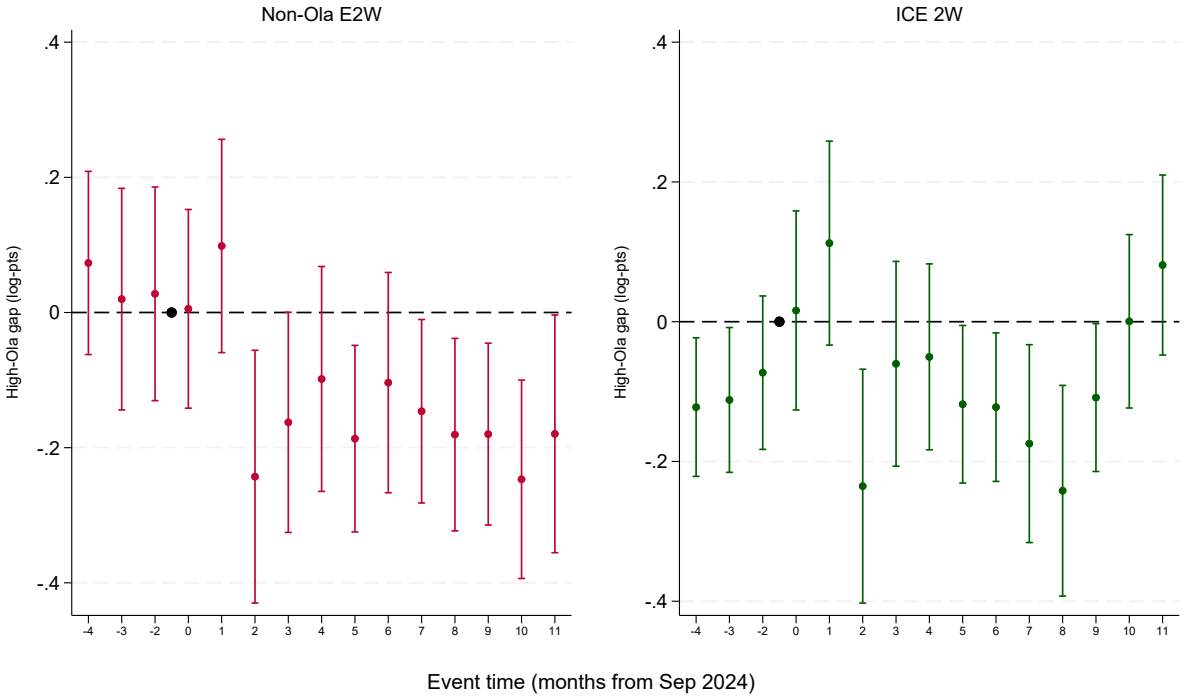
Segment	Observed registrations	National counterfactual	Estimated shortfall
Non-Ola electric two-wheelers	643,617	756,454	112,837
ICE two-wheelers	7,176,661	7,212,972	36,311
Total (non-Ola electric + ICE)	7,820,278	7,969,426	149,148

Panel B. Registration differences under alternative counterfactuals

	Counterfactual segment trends		
	National	Regional	State
Non-Ola electric shortfall	112,837	52,077	59,099
	[46,500, 181,364]	[-2,104, 107,929]	[20,290, 98,917]
Excess ICE registrations	-36,311	123,088	134,185
	[-596,040, 493,420]	[-267,908, 501,655]	[-154,823, 419,604]
Residual net shortfall	149,148	-71,010	-75,086
	[-396,896, 742,411]	[-462,603, 339,026]	[-365,971, 223,185]

Notes: PPML estimates from Equation (A.1) for non-Ola electric and ICE two-wheelers over May 2024–August 2025. High exposure denotes the top exposure quartile. Counterfactual predictions follow Equation (A.2). Panel A uses national segment $\times$ month effects; its total sums the two reported segments. Panel B replaces these monthly effects with regional or state segment $\times$ month effects in the corresponding columns. The electric shortfall is counterfactual minus observed registrations; excess ICE registrations are observed minus counterfactual. The residual subtracts excess ICE registrations from the electric shortfall. It does not measure delayed or forgone purchases. Brackets report 95% intervals derived from the coefficient sampling distribution, with two-way clustering by RTO and state $\times$ month. Entries are rounded independently.

Figure A-9: Event-study registration gaps by vehicle segment



Notes: Event-study coefficients $\theta_{f\tau}$ on $High_r \cdot \mathbf{1}[t - \text{Sep } 2024 = \tau] \cdot \mathbf{1}[f]$ for the non-Ola electric and ICE segments, relative to August 2024, from the stacked PPML model with RTO $\times$ segment and segment $\times$ month fixed effects and segment-specific $B_r \cdot Post$ controls. The outcome is registration counts; coefficients measure changes in log expected registrations. Error bars are 95% confidence intervals based on standard errors clustered by RTO and state $\times$ month. The non-Ola electric segment has a comparatively flat pre-period and negative post-period coefficients, while the ICE coefficients fluctuate around zero.